Chapter 5

Results and discussions

This chapter is concerned with a capability and restrictions of the Bayesian method to calculate the mobility spectrum. This chapter is divided into 3 sections. In the first section, the Bayesian method with Entropic prior is performed on synthetic data under varying conditions. The purpose is to test a stability of the solution depending on adjustable parameters in the algorithm. Then the developed program is performed on the experimental data in order to study the temperature-dependent electrical transport of a Ge/SiGe heterostructure. In the last section, an error analysis is studied. The conductivity uncertainty is examined with some influential factors.

5.1 Synthetic data

The synthetic data of Hall coefficient and resistivity are generated from two carrier species: $\mu_1 = 2,000$ $cm^2V^{-1}s^{-1}$, $n_1 = 1 \times 10^{11}$ cm^{-2} and $\mu_2 = 6,000$ $cm^2V^{-1}s^{-1}$, $n_2 = 1 \times 10^{11}$ cm^{-2}. The data are generated for 400 points of magnetic field equally spaced from 0.1 to 10 Tesla. Carrier species No. 1 and 2 are superimposed by normal distribution with standard deviations of 250 and 500 $cm^2V^{-1}s^{-1}$ respectively. The details are summarized in Table 5.1. Fig. 5.1 illustrates the true mobility spectrum of a conductivity in an arbitrary unit versus mobility. Fig. 5.2 shows the Hall coefficient and magnetoresistivity versus magnetic field. The Hall co-

efficient decreases monotonically with increasing magnetic fields while the resistivity has a reverse trend.

Noise in measurement is considered. Although there are many sources of errors in a real situation, for simplicity, the noise is assumed to be Gaussian noise and exists only in longitudinal and transverse (Hall) voltages. The magnitude of noise is defined as a standard deviation of the Gaussian distribution, which is a percentage of the measured voltage at any magnetic field strength. The Gaussian error in Hall and resistivity data is propagated into the conductivity data by the error propagation formula in Eq. (4.31). Other details and the formulation of conductivity error propagation are in Appendix A. Fig. 5.3 shows the normalized longitudinal and transverse components of conductivity tensor with varying magnetic fields, and the structure of conductivity error is shown in Fig. 5.4.

Table 5.1 The detail of synthetic model for algorithm testing.

Species	Mobility ($cm^2V^{-1}s^{-1}$)	Mobility standard deviation ($cm^2V^{-1}s^{-1}$)	Concentration (cm^{-2})
Hole#1	2,000	250	1×10^{11}
Hole#2	6,000	500	1×10^{11}

5.1.1 Calculation setting

To calculate the mobility spectrum for a given set of synthetic data defined in Section 5.1, the method described in Section 4.4 is followed. The standard deviation of Gaussian noise is defined to 0.1%. The number of magnetic field points (M) is selected to be 100 points spaced equally over the magnetic field range. The number of mobility points (N) in mobility spectrum is set to 50 points covering the mobility range from +100 to +10,000 $cm^2V^{-1}s^{-1}$ for holes and from -100 to -10,000 $cm^2V^{-1}s^{-1}$ for electrons. The Markov chain is generated by a random walk in N dimensions. The proposal distribution of the Markov chain (see Section 4.6

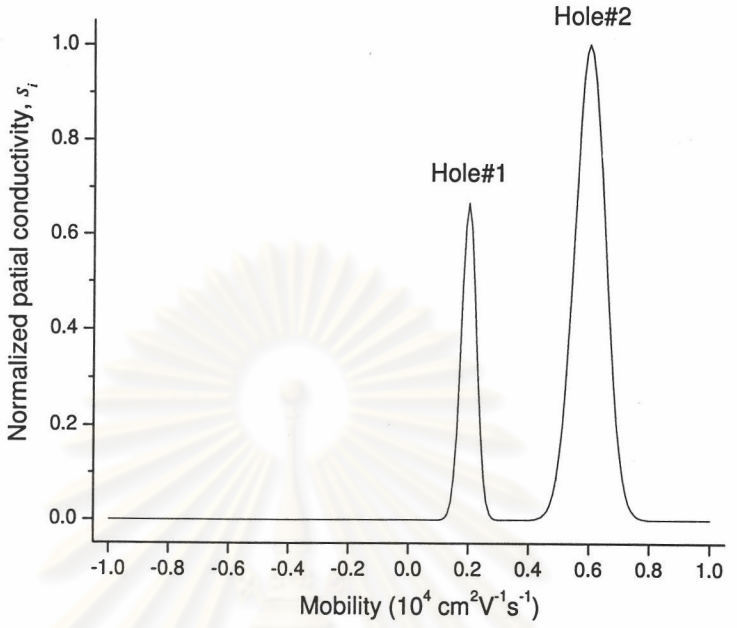

Figure 5.1: The synthetic mobility spectrum of two-hole carrier species (n_1=1×10^{11} cm^{-2}, μ_1=2,000 $cm^2V^{-1}s^{-1}$, n_2=1×10^{11} cm^{-2}, μ_2=6,000 $cm^2V^{-1}s^{-1}$ with standard deviations of 250 and 500 $cm^2V^{-1}s^{-1}$, respectively).

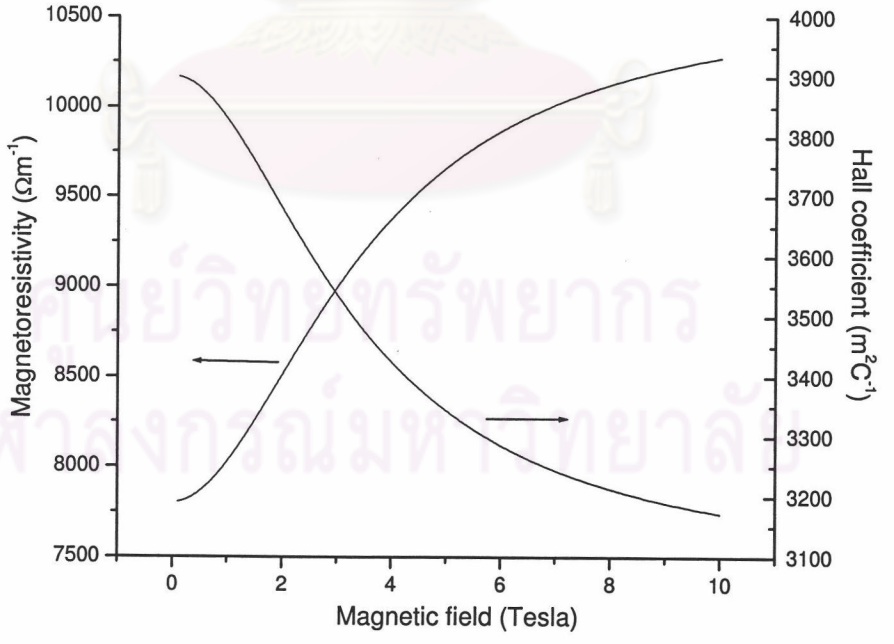

Figure 5.2: Hall coefficient and magnetoresistivity versus magnetic field for synthetic mobility spectrum in Fig 5.1.

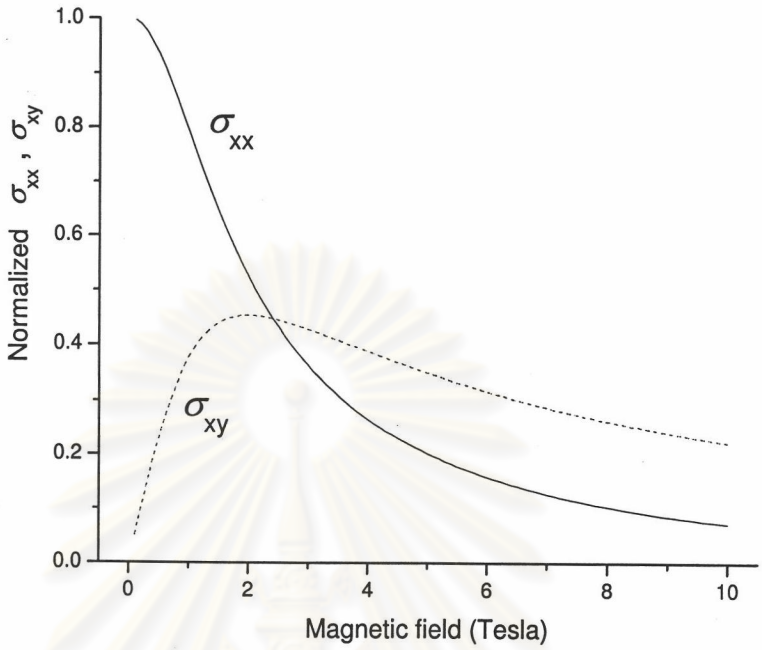

Figure 5.3: The longitudinal (σ_{xx}) and transverse (σ_{xy}) components of conductivity tensor in normalized unit versus magnetic field.

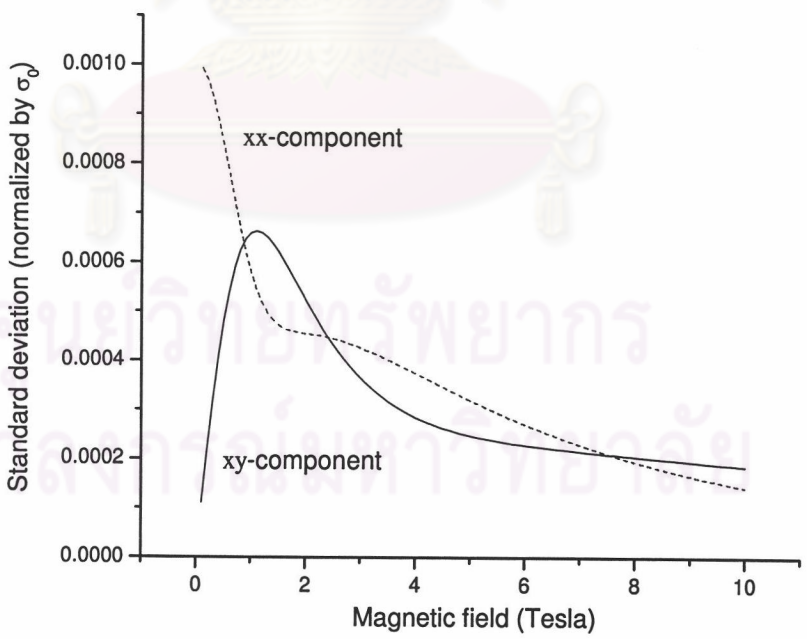

Figure 5.4: The 0.1% Gaussian noise of normalized longitudinal (σ_{xx}) and transverse (σ_{xy}) components of conductivity tensor versus magnetic field.

for details) is a normal distribution of zero mean and unit variance multiplied with a weight factor ω of 1.25% to the current magnitude of the partial conductivity in mobility spectrum. For the likelihood function, the standard deviation defined for χ^2 is usually assigned to the same magnitude of noise in order to yield the best fitting, at which χ^2 approximately equals to the number of data ($2M$). For example, 0.1% s.d. is defined to the synthetic data with 0.1% Gaussian noise. For the entropic prior, the default model $\{m_i\}$ is defined to a flat distribution which is used for all data set in this thesis. The initial value of α is set to 900 for the calculation of about 2,000,000 to 3,000,000 iterations (see Step 1 in Appendix B). By further iterations (Step 2), the α is decreased by a factor of 0.9 for every successive 200,000 iterations until the best fit is yielded. The parameter α is then manually stopped decreasing, and the calculation continues for another 2,000,000 iterations or higher to collect the set of most probable spectra. Details are summarized in Table 5.2.

Table 5.2 The parameter setting for the calculation of the mobility spectrum for a given data in Table 5.1.

Configuration	Value	Range/Remark
# magnetic field points (M)	100	0.1 to 10 Tesla
# mobility points (N)	50	+100 to +10,000 $cm^2V^{-1}s^{-1}$ for hole and -100 to -10,000 $cm^2V^{-1}s^{-1}$ for electron
Default model $\{m_i\}$	Flat	
Initial α	900	
Decreased factor	0.9	every 200,000 iterations
Weight factor ω	1.25%	of partial conductivity
Noise (s.d.)	0.1%	of conductivity data
s.d. in likelihood	0.1%	
Stopped α	any	until $\chi^2 \approx 2M$

5.1.2 Selection of stopped alpha

As described in Section 4.4, the decreasing of α is stopped when χ^2 approximately saturates at $2M$. At this point, the peaks appear clearly in the mobility

spectrum. This is the situation where the entropy of spectrum is the highest while χ^2 is the lowest, according to the maximum entropy principle. In practical, however, the spectrum sometimes collapses even when the χ^2 has not yet saturated. In addition, it is hard to seek a certain saturated value of χ^2 because χ^2 fluctuates due to the nature of the random process.

The following section will show that it is unnecessary to look for the stopped value of α precisely. A wide choice of α which is around the saturated point of χ^2 is acceptable. To clarify the statement, the Bayesian method was performed on synthetic data in Section 5.1 with 0.1 % Gaussian noise. The calculation configuration is shown in Table 5.2. The initial value of α is 900. The computer program was run to form the smooth spectrum and then α was decreased with a factor of 0.9. The decreasing α was stopped at some selected values. The stopped value was defined differently from 900 to 5 (see Table 5.3). Figs. 5.5 (a) and 5.5 (b) show the Hall mobility and concentration with corresponding error bars of each carrier species extracted from the mobility spectrum at different values of α. From Fig. 5.5 (a), the mobility of Hole#1 fluctuates around the value of 2,000 $cm^2V^{-1}s^{-1}$, and that of Hole#2 converges to some certain value close to 6,000 $cm^2V^{-1}s^{-1}$ where α is less than 125. The error bar of mobility of two species at each α do not change with α significantly, but the error bars at small α's (15 and 5) are relatively small. This is due to a low acceptance rate in MCMC sampling. The concentration in Fig 5.5 (b) expresses the same characteristic as that of mobility. The concentration converges to the correct value where the stopped value of α becomes close to the value at the saturated χ^2. We can conclude that the solution is only slightly different from the correct one, even though the stopped α is doubly different from the best value (saturated value). Table 5.3 shows the χ^2, H and their corresponding standard deviation at different stopped α's.

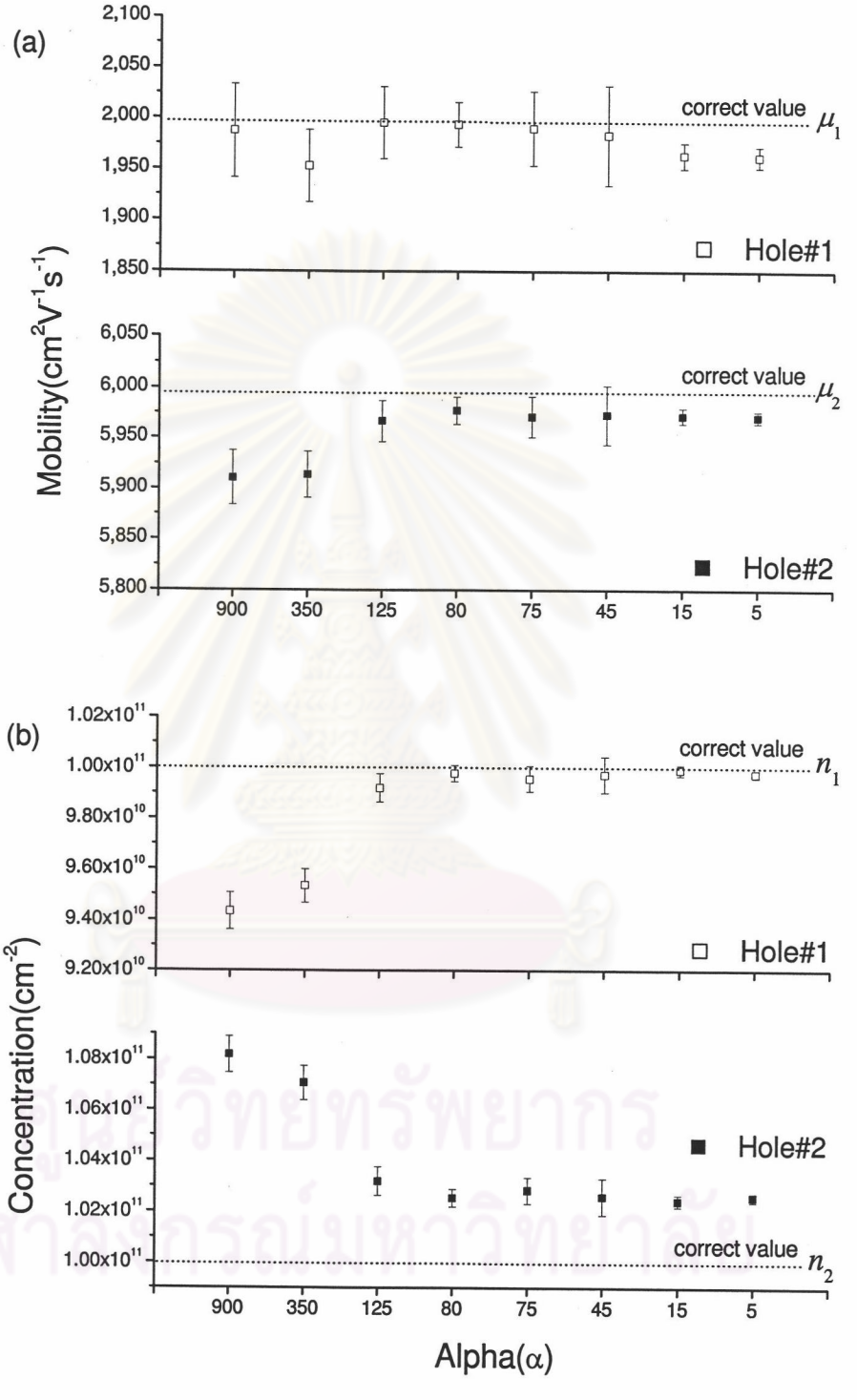

Figure 5.5: (a) Hall mobility and (b) concentration of Hole#1 and Hole#2 species at different stopped α. Dash lines present the correct values.

Table 5.3 The chi-square and entropy of mobility spectra at different α's

Stopped α	χ^2	σ_{χ^2}	H	σ_H
900	444.159	24.459	-1.288	0.014
350	262.098	12.186	-1.474	0.021
125	203.496	5.678	-1.679	0.028
80	197.548	4.848	-1.769	0.035
75	194.378	3.617	-1.798	0.025
45	194.212	3.768	-1.793	0.045
15	190.678	2.364	-2.208	0.080
5	191.025	2.690	-2.525	0.024

5.1.3 Random generator

The MCMC algorithm is strongly related to the random process. To apply the algorithm, there are several points to consider such as the proposal distribution (see Section 4.6), the updating order, the number of chains and starting values (see Gilks et al. (1995) for more details). In this section, designing of the proposal distribution and a random sequence are concerned. According to the Markov process, these factors do not affect a solution if they are used carefully. To ensure the correctness of theoretical aspect, the effect of proposal distribution and random sequence to the mobility spectrum are investigated.

Proposal distribution

By MCMC algorithm, the Markov chain is generated as a random walk in N dimensions where N is a number of parameters. For our problem, it is the number of mobility points in a spectrum. For each mobility point, the partial conductivity is updated randomly by the following relation:

$$s_i^{new} = s_i^{old} \times (1 + \omega \times N(0,1)). \tag{5.1}$$

The $N(0,1)$ is a normal distribution with zero mean and unit variance. The ω is an arbitrary positive parameter used to define the magnitude of standard deviation of

$N(0,1)$. Eq. (5.1) guarantees a non-negative partial conductivities for all iterations (sampling). Eq. (5.1) is also easy to evaluate with only multiplication operator. In this updating form, the proposal distribution is the normal distribution with mean of the current value of the partial conductivity and standard deviation of the current partial conductivity multiplying with ω. So, there are many available proposal distributions depending on ω. The form of a proposal distribution does not affect the final solution if the Markov chain already converges to its equilibrium state. However, the rate of convergence to the equilibrium state depends significantly on the relation between the proposal distribution and the target distribution. In addition, the Markov chain may poorly contribute to the target distribution even having convergence. All unsuitable proposal distributions cause large computing time.

The problem is to find a suitable ω used in Eq. (5.1). To study the effect of the factor ω to the solution, a Bayesian program is performed with varying ω's on the same synthetic data. The parameter ω is set to 0.008, 0.01, 0.0125, and 0.014. Fig. 5.6 illustrates the mobility spectra obtained from different ω's. All spectra are collected at $\alpha = 45$. Figs. 5.7 (a) and 5.7 (b) show solutions at different ω's. From both Figs. 5.6 and 5.7, we can see that the mobility spectra, Hall mobility and concentration of two hole species are not significantly different. Table 5.4 shows the acceptance rate of all ω's. The acceptance rate is decreased with increasing ω but they are on the reasonable rate. In summary, the acceptance rate is low if ω is large when compared to the width of the target distribution and the convergence is hardly obtained. A very low acceptance rate gives a small set of sampling spectra that may make a statistical test failed. Even though the set of probable spectra is large when ω is small, we observed a relatively slow formation of the mobility spectrum. Therefore, for all data set in this thesis, the ω will be set to 0.0125 which means that the standard deviation of the proposal distribution is 1.25% of

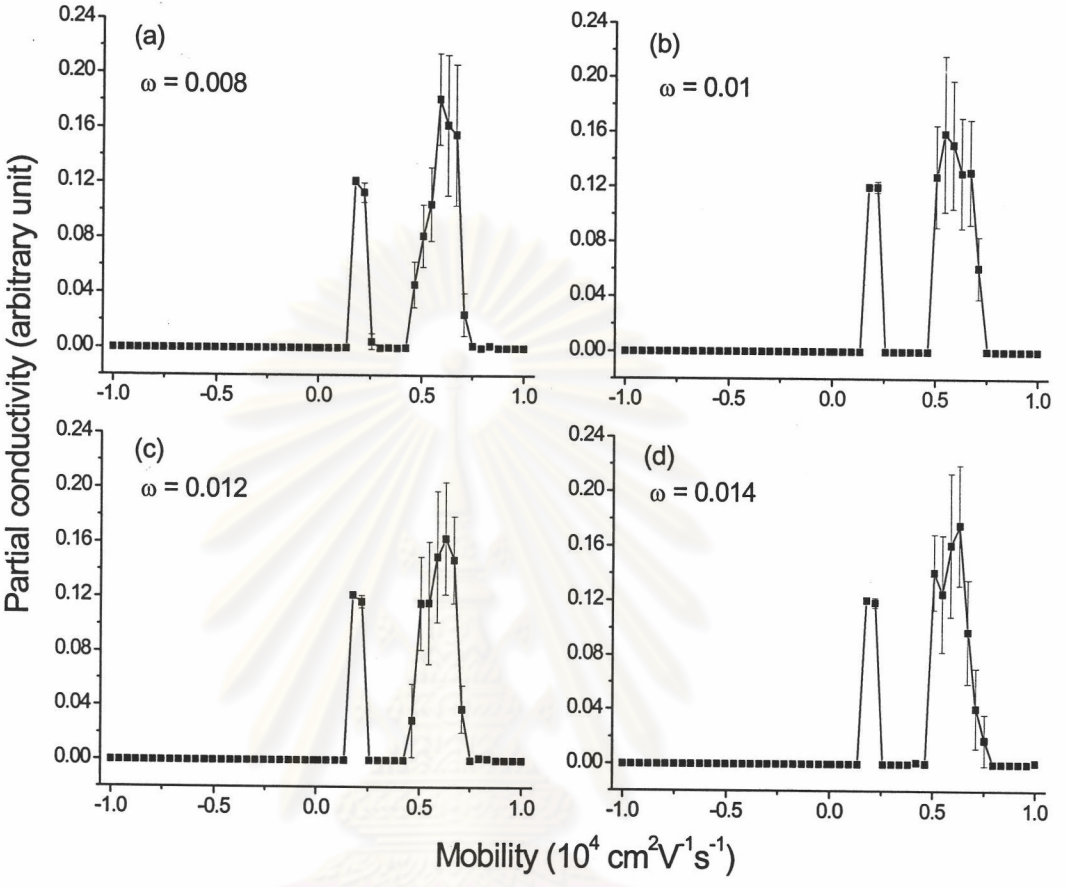

Figure 5.6: Bayesian spectra of synthetic data at different ω's (a) 0.008, (b) 0.01, (c) 0.012, and (d) 0.014.

ศูนย์วิทยทรัพยากร
จุฬาลงกรณ์มหาวิทยาลัย

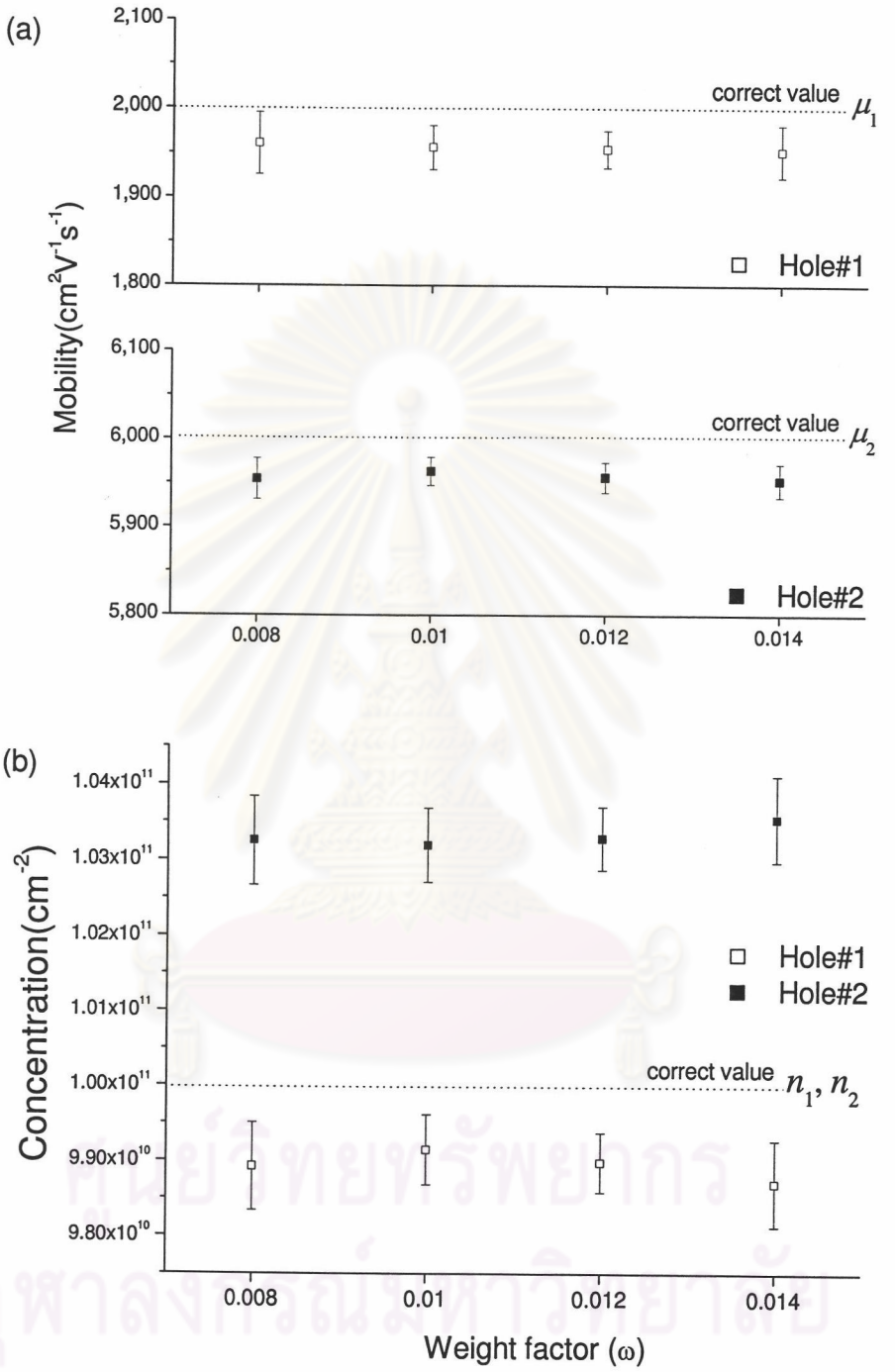

Figure 5.7: (a) Hall mobility and (b) concentration of Hole#1 and Hole#2 species at different ω's.

the current magnitude of the partial conductivity.

Table 5.4 The chi-square, entropy and acceptance rate of mobility spectra at different ω's.

ω	χ^2	σ_{χ^2}	H	σ_H	Acceptance (%)
0.008	193.143	3.311	-1.848	0.022	4.59
0.010	192.714	3.128	-1.823	0.034	3.36
0.012	190.872	2.533	-1.887	0.041	2.59
0.014	191.622	2.839	-1.863	0.041	1.97

Initial Seed number

The normal distribution generators used in the developed program are from Press et al. (1986), namely *ran*1 () and *gasdev* (). The routines return a number randomly with the normal deviation of zero mean and unit variance. The routines require a negative integer so called "seed number" at the beginning of the calculation. The seed number is used to assign the initial value of a random sequence. A different seed number provides a different random sequence. In principle, every different random sequences should produce the same statistical results. In other words, a good program should be less sensitive to the choice of different random sequences. The sensitivity of the developed program to initial seed number is demonstrated by performing the program with different seed numbers on the same synthetic data set. Five different sequences of Markov chain are generated to represent the same mobility spectrum. The results are shown in Figs. 5.8 and 5.9. Fig. 5.8 illustrates the mobility spectra from different random sequences, which are considerably similar in shape. The Hall mobility and carrier concentration of Hole#1 and Hole#2 species in Figs. 5.9 (a) and 5.9 (b), respectively, are also insignificantly different. The χ^2, H, and acceptance rate of all spectra are given in Table 5.5. This indicates that the developed program is insensitive to the choice of the random sequences as it should be.

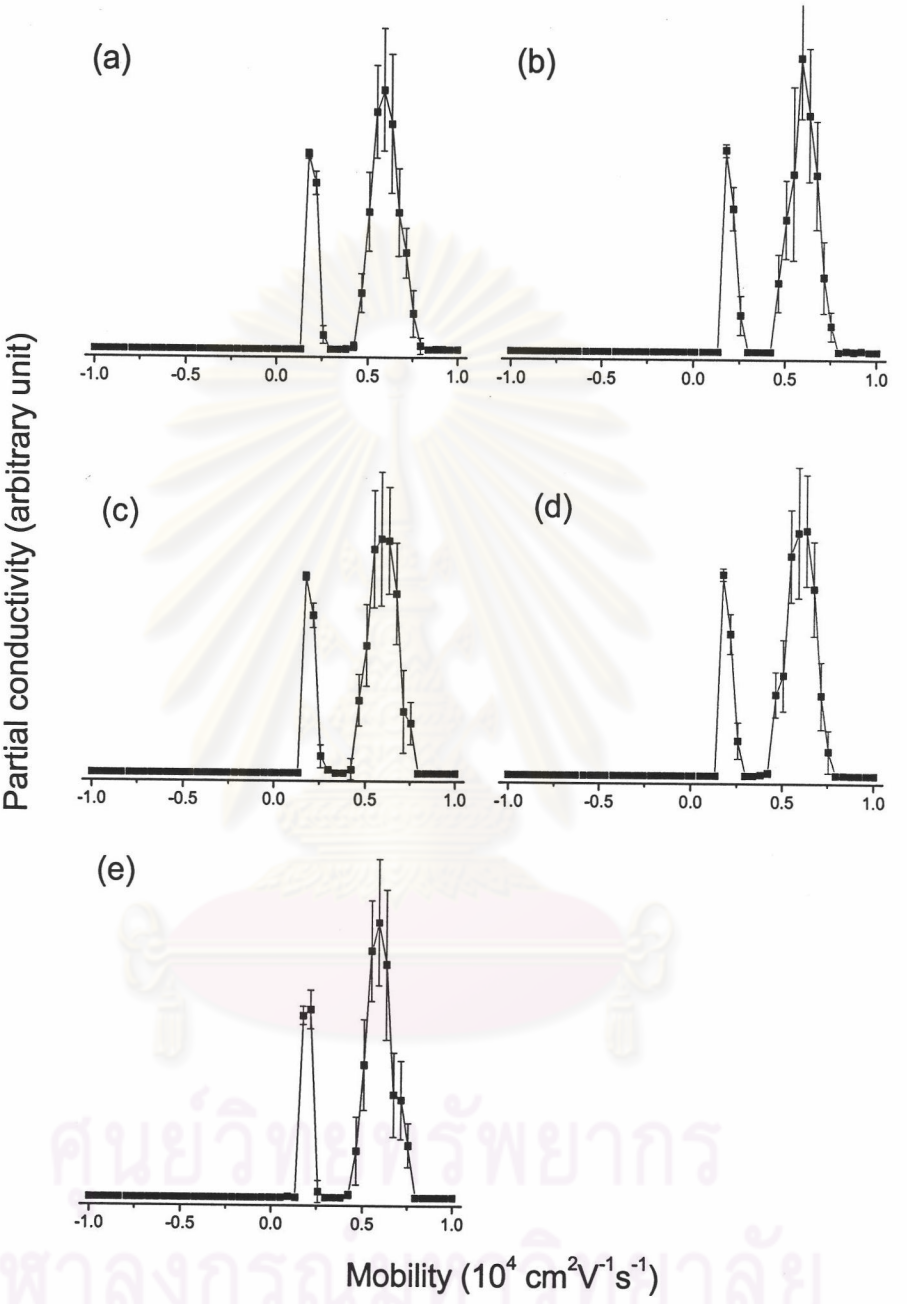

Figure 5.8: Bayesian spectra of synthetic data at different initial seed number. α is 75.

ศูนย์วิทยทรัพยากร
จุฬาลงกรณ์มหาวิทยาลัย

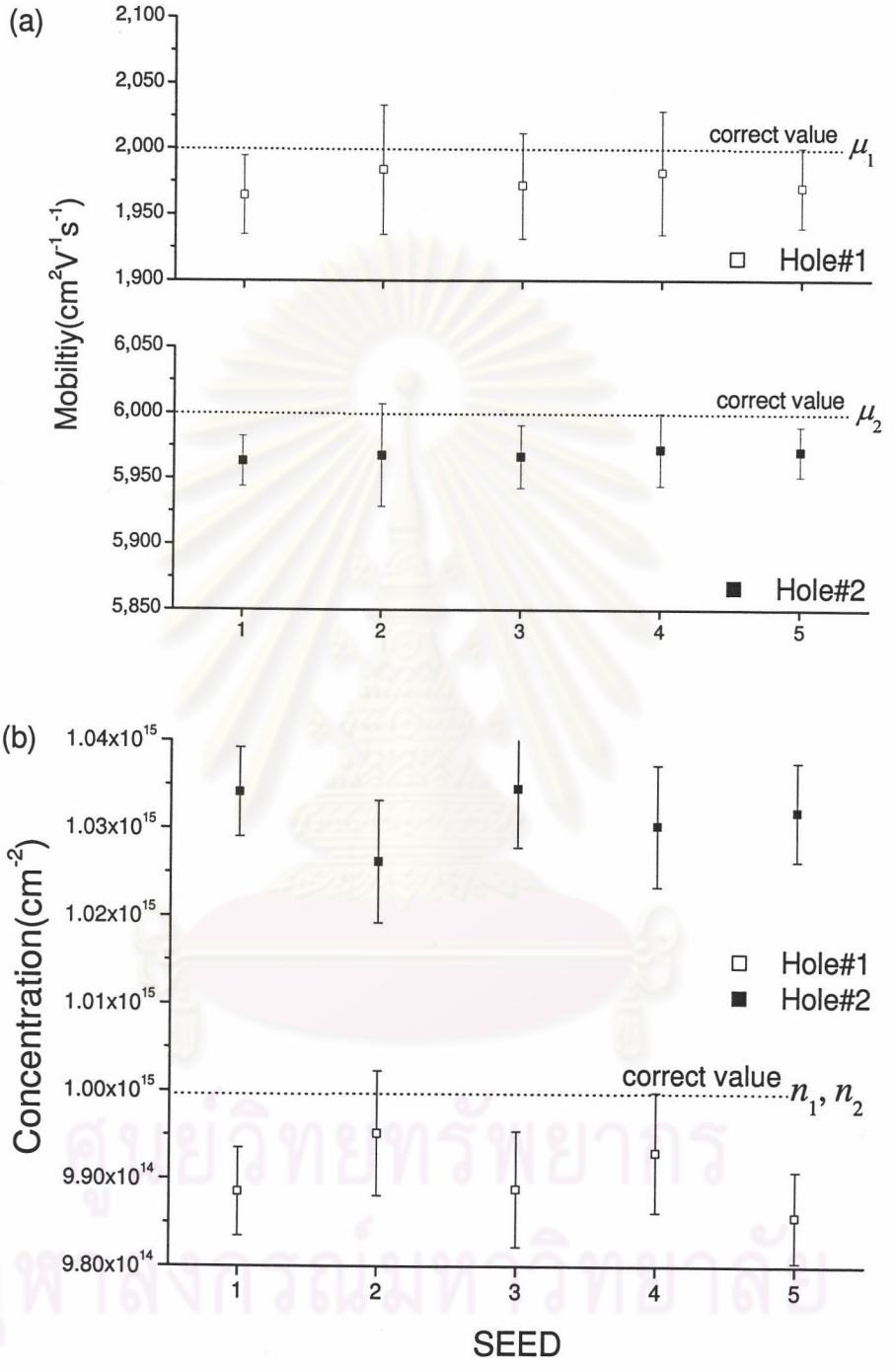

Figure 5.9: (a) Hall mobility and (b) concentration of Hole#1 and Hole#2 species at different initial seed numbers.

Table 5.5 The chi-square, entropy and acceptance rate of mobility spectra at different seed numbers.

Number	χ^2	σ_{χ^2}	H	σ_H	Acceptance (%)
1	196.664	2.351	-1.704	0.030	2.45
2	196.960	2.220	-1.722	0.025	2.41
3	198.183	2.104	-1.705	0.019	2.39
4	196.560	2.035	-1.707	0.020	2.41
5	198.646	2.810	-1.738	0.054	2.40

5.1.4 Incomplete data

From the experimentalist view point, data can be incomplete in many ways such as the low data points density and the high level of noise. In mobility spectrum problem, the maximum value of magnetic field is included. The data imperfection causes poor inference. This section is devoted to studies of the effect of these factors to mobility spectrum calculation through the Bayesian method.

Density of data

Problem size is one of the factors that affects the calculation time. "Size" means a number of measured data and a number of mobility points in spectrum. Even though decreasing a number of data points reduces a calculation time, it increases a degree of incompleteness. In a well-defined situation, a number of data points is greater than a number of parameters. In this section, we use synthetic data as described in Section 5.1. The mobility spectrum calculation is performed on the same synthetic data for 6 times. Each time, the number of magnetic field points (M) is selected to 75, 50, 25, 20 and 15 points. All set of data cover the same magnetic field range of 0.1 to 10 Tesla, and data points are chosen uniformly. The number of mobility points N is fixed to 50. The resultant spectra are shown in Fig. 5.10. The two hole species are observed and the peaks are well separated. The peak of Hole#2 in the mobility spectrum becomes less smooth as the number

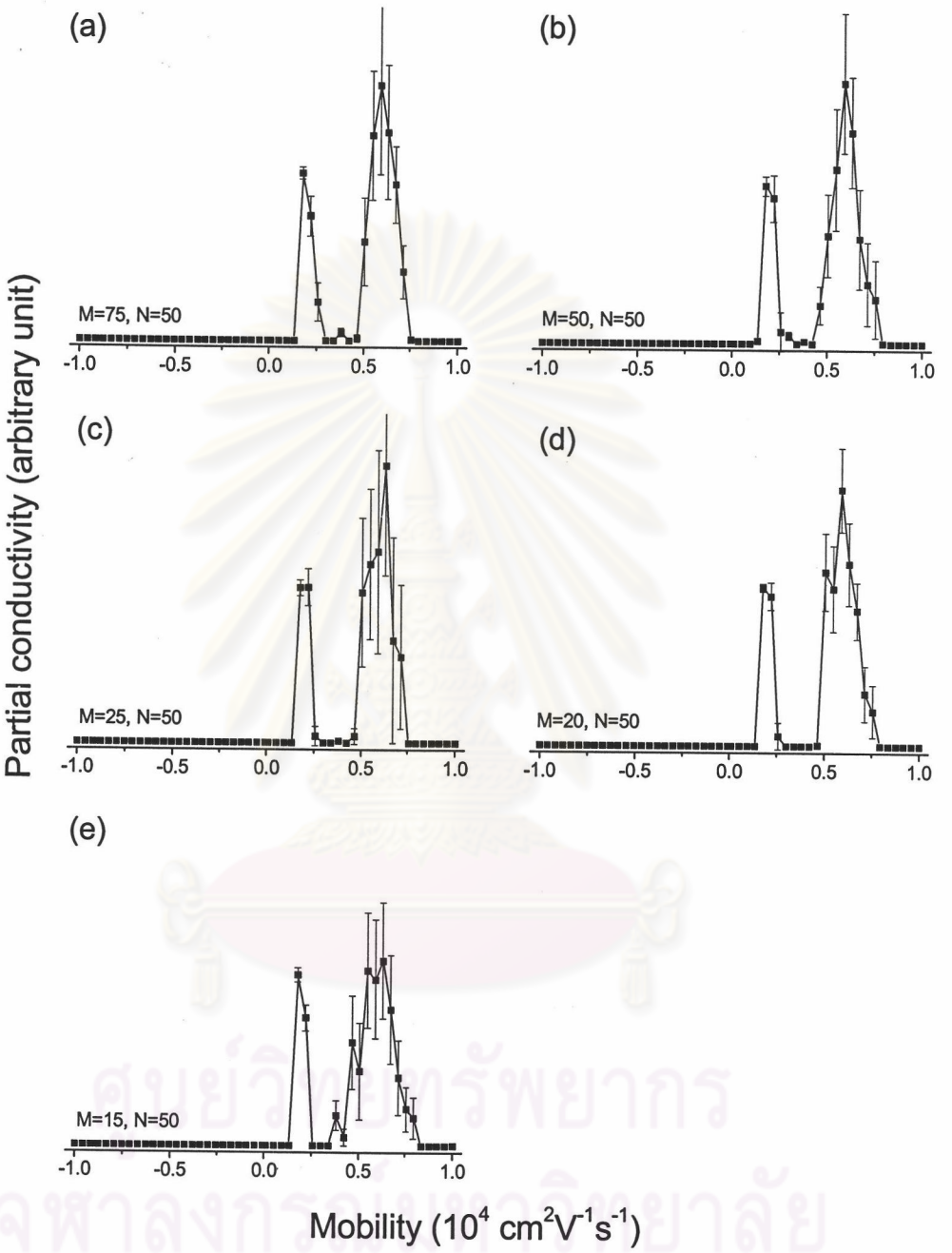

Figure 5.10: Bayesian spectra of synthetic data of different number of magnetic field points (M). A number of mobility points (N) is fixed to 50.

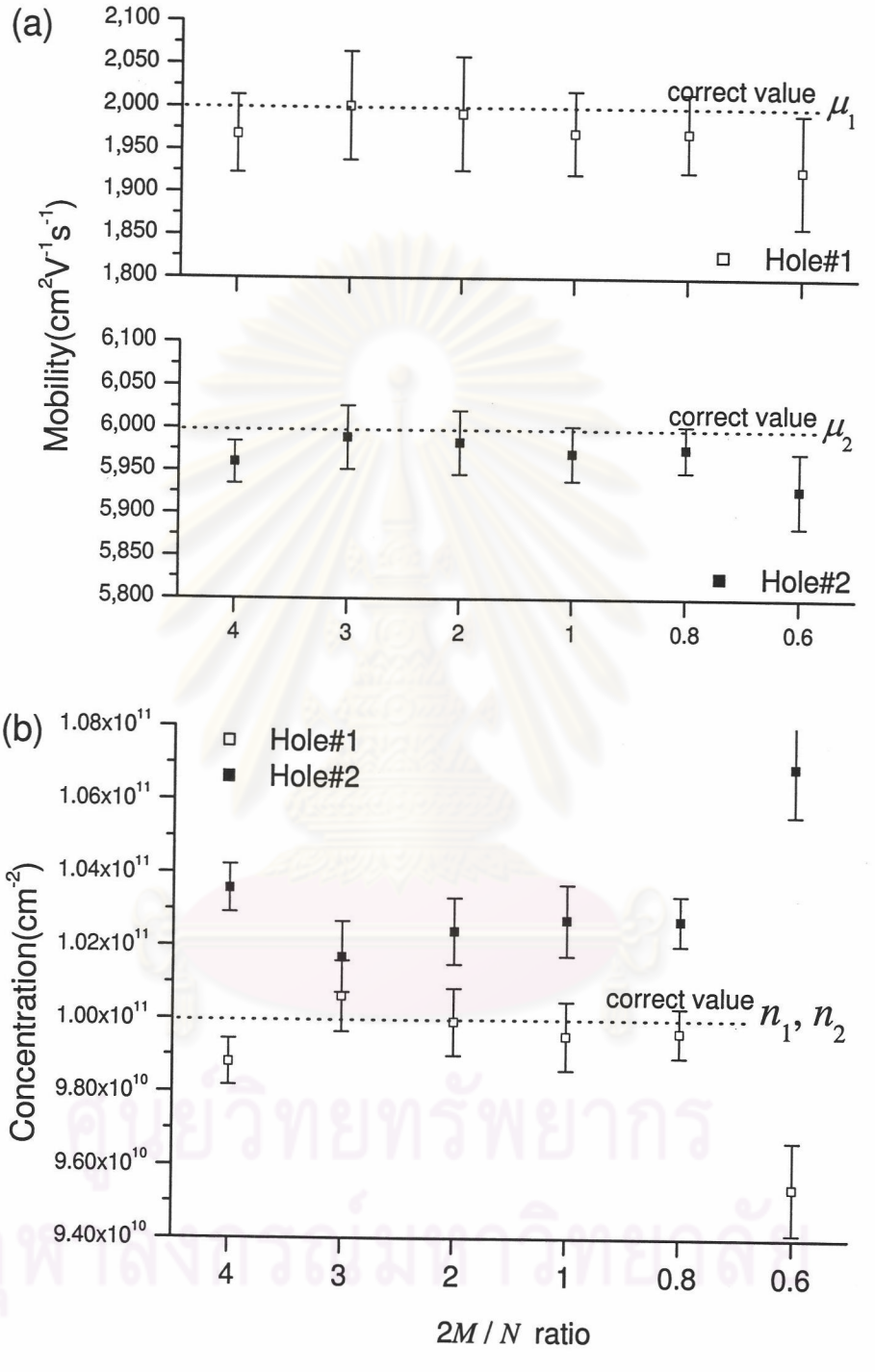

Figure 5.11: (a) Hall mobility and (b) concentration of Hole#1 and Hole#2 species at different ratio of a number of data points ($2M$) to a number of mobility points (N).

of data points is decreased. Fig 5.11 (a) shows the Hall mobility with error bars of each set of data. The Hall mobility of two hole species for M=15 $\left(\frac{2M}{N} = 0.6\right)$ shifts to the lower mobility than others. The results are the same for Hall conductivity shown in Fig. 5.11 (b). Considering Table 5.6, the χ^2 decreases by decreasing the number of data points, and the increasing of acceptance rate is observed. Although the results are acceptable, we suggest that one should use all available data with the ratio $\frac{2M}{N} \geq 0.8$.

Table 5.6 The chi-square, entropy and acceptance rate of mobility spectra at different number of data points.

$2M$ to N Ratio	χ^2	σ_{χ^2}	H	σ_H	Acceptance (%)
3 (M=75)	130.78	3.44	-1.836	0.052	3.06
2 (M=50)	100.23	3.64	-1.754	0.070	4.26
1 (M=25)	38.91	2.96	-1.989	0.085	6.35
0.8 (M=20)	37.16	3.63	-1.717	0.059	7.94
0.6 (M=15)	42.07	4.77	-1.602	0.051	9.43

Maximum magnetic field

According to the characteristic of the problem, μB condition plays an important role in mobility spectrum analysis. The μB is the multiplication between the lowest value of Hall mobility in the sample with maximum magnetic field strength. The ability to infer the lowest-mobility species depends on the maximum magnetic field strength provided by the instrument. The critical value of $\mu B = 1$ is the point where the mobility spectrum is strongly related to the data [Dzuiba(1990)]. For example, in the 10 Tesla measurement, the lowest mobility that can be identified is 1,000cm^{2}V^{-1}s^{-1} (10^{-1} m^{2}V^{-1}s^{-1}). To answer the question how the μB affects the spectrum, the calculation is performed on the synthetic data with different maximum magnetic fields between 10 to 2.5 Tesla. The number of data points is selected to 100 points equally for all data set. This synthetic data has a minimum value

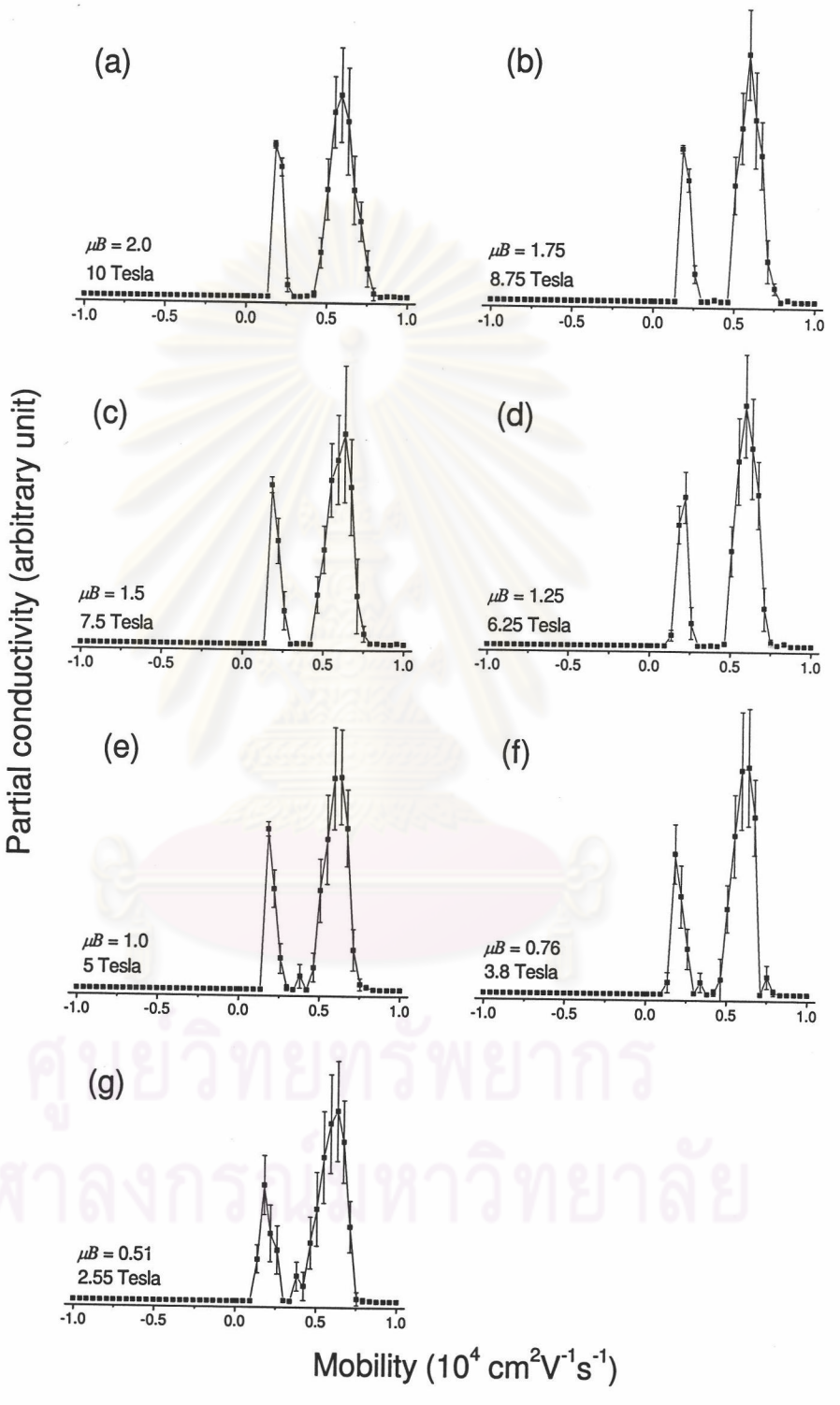

Figure 5.12: Bayesian spectra of synthetic data of different maximum magnetic field strengths. The maximum strength is decreased form 10 Tesla to 2.5 Tesla.

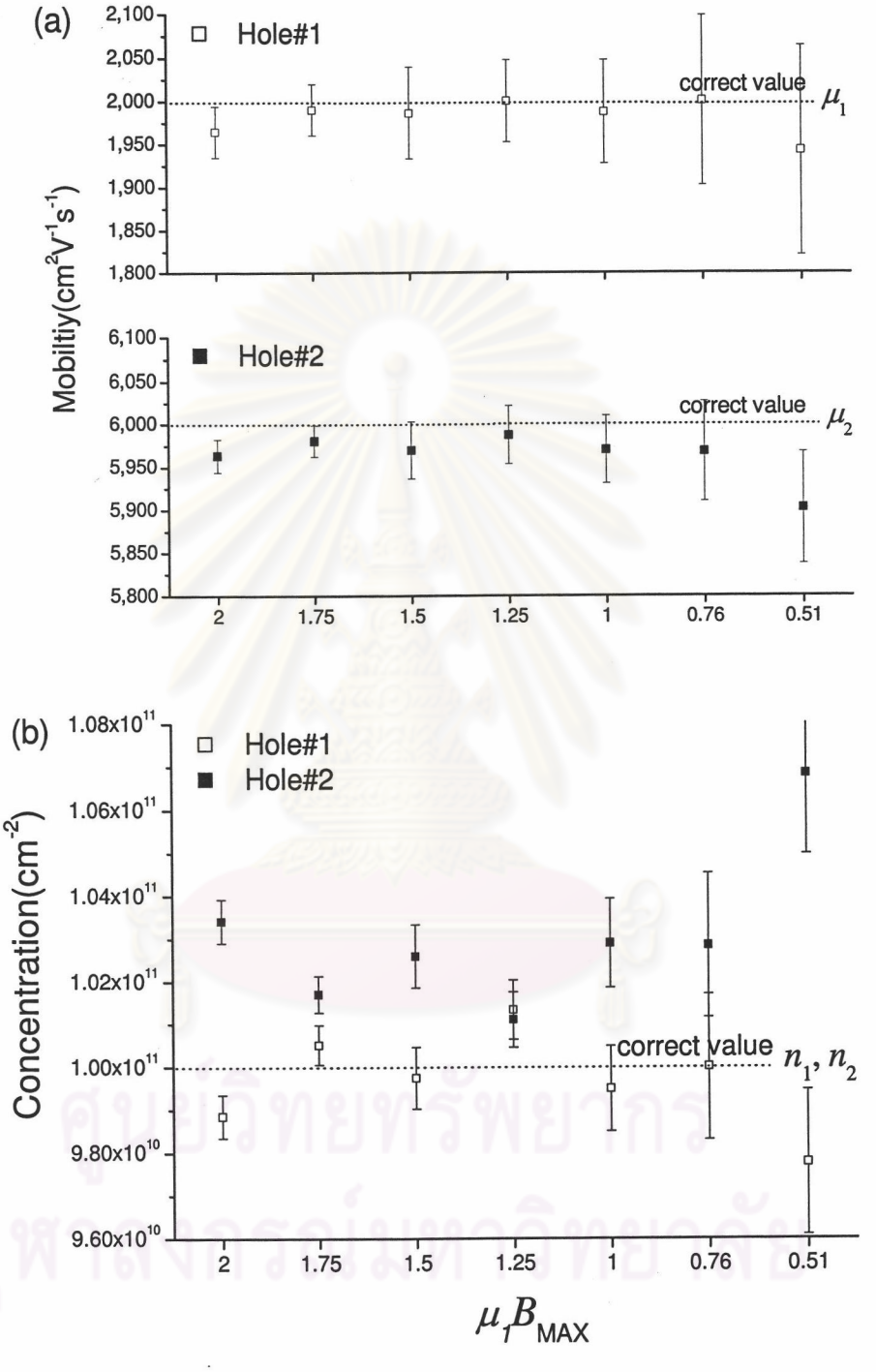

Figure 5.13: (a) Hall mobility and (b) concentration of Hole#1 and Hole#2 species at different $\mu_1 B_{MAX}$. Relative large error bars are observed for small value of $\mu_1 B_{MAX}$. $\mu_1 = 2{,}000\ cm^2V^{-1}s^{-1}$.

of Hall mobility at 2,000 $cm^2V^{-1}s^{-1}$. Then, the μB is varied from about 0.5 to 2. Fig. 5.12 shows the resultant mobility spectra when the maximum magnetic field strength is reduced. It is found that as maximum strength decreases the quality of spectrum becomes poorer. The results at $\mu B > 1$ present good spectra with well separated peaks of the hole species. At $\mu B \leq 1$ the mobility spectrum distorts by small transient peaks with relatively large error bars. It is hard to decide in the real situation whether these small peaks are real ones or just artifacts.. Figs. 5.13 (a) and 5.13 (b) show the Hall mobility and concentration value of the Hole#1 and Hole#2. At $\mu B \lesssim 1$, their error bars are relatively large and the Hall mobility and concentration are significantly incorrect. From Table 5.7, we also observed that the acceptance rate increases with the decreasing μB.

Table 5.7 The chi-square, entropy and acceptance rate of mobility spectra at different μB.

μB	χ^2	σ_{χ^2}	H	σ_H	Acceptance (%)
2.00	196.664	2.351	-1.704	0.030	2.45
1.75	238.415	4.392	-1.811	0.041	2.58
1.50	210.189	4.321	-1.740	0.039	2.77
1.25	170.106	5.236	-1.831	0.037	3.16
1.00	170.106	5.236	-1.831	0.037	3.50
0.76	213.832	4.691	-1.796	0.047	4.47
0.51	197.705	5.624	-1.588	0.041	6.74

Noise in data

The most interesting factor that affects the mobility spectrum calculation is noise associated with the measured data. Noise does not only distort the shape of spectrum, but sometimes it leads to misinterpretation of a number of existing carrier species. The effect of noise is demonstrated by performing the calculation with varying degrees of noise. The Gaussian noise of 0.05%, 0.1%, 0.25%, and 0.5% are added to synthetic data. The standard deviation of chi-square terms in likelihood

distribution are set to the same value. The resultant spectra are in Fig. 5.14 which shows the decreasing in peak quality as the noise level is increased. Considering the Hall mobility at different level of noise in Fig 5.15 (a), the error bar of the mobility is large for high noise levels. The same observation appears for the case of Hall concentration in Fig. 5.15 (b). From Table 5.8, it is found that the fitting to data of all cases is almost the same, but the shape of spectrum is significantly different. The acceptance rate is also increased as the level of noise increases.

Table 5.8 The chi-square, entropy and acceptance rate of mobility spectra at different levels of noise.

Noise(%)	χ^2	σ_{χ^2}	H	σ_H	Acceptance (%)
0.05	198.798	5.406	-1.77	0.037	0.68
0.10	196.664	2.351	-1.70	0.030	2.45
0.25	193.686	3.914	-1.67	0.055	9.18
0.50	194.225	3.324	-1.62	0.058	19.48

In conclusion, three types of incomplete data are examined. It can be summarized that the imperfection of data affects the spectrum shape, the calculated mobility and concentration.

ศูนย์วิทยทรัพยากร
จุฬาลงกรณ์มหาวิทยาลัย

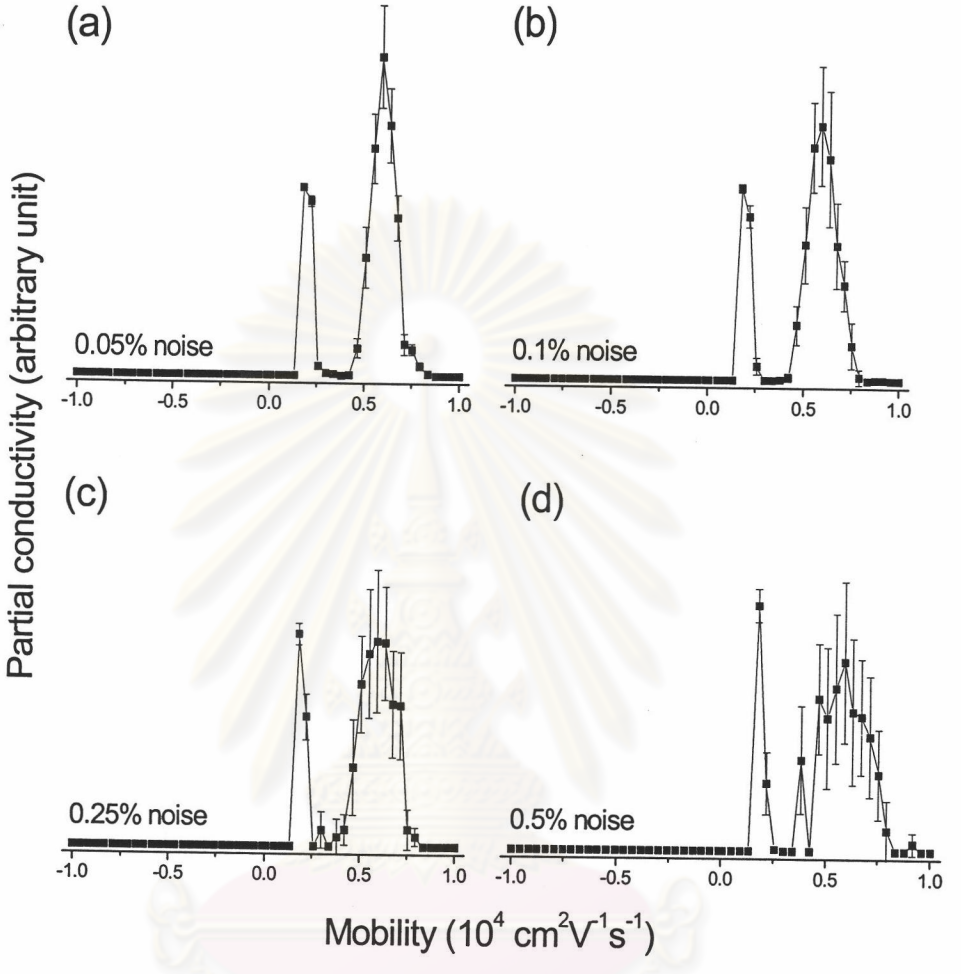

Figure 5.14: Bayesian spectra of synthetic data at different levels of noise.

ศูนย์วิทยทรัพยากร
จุฬาลงกรณ์มหาวิทยาลัย

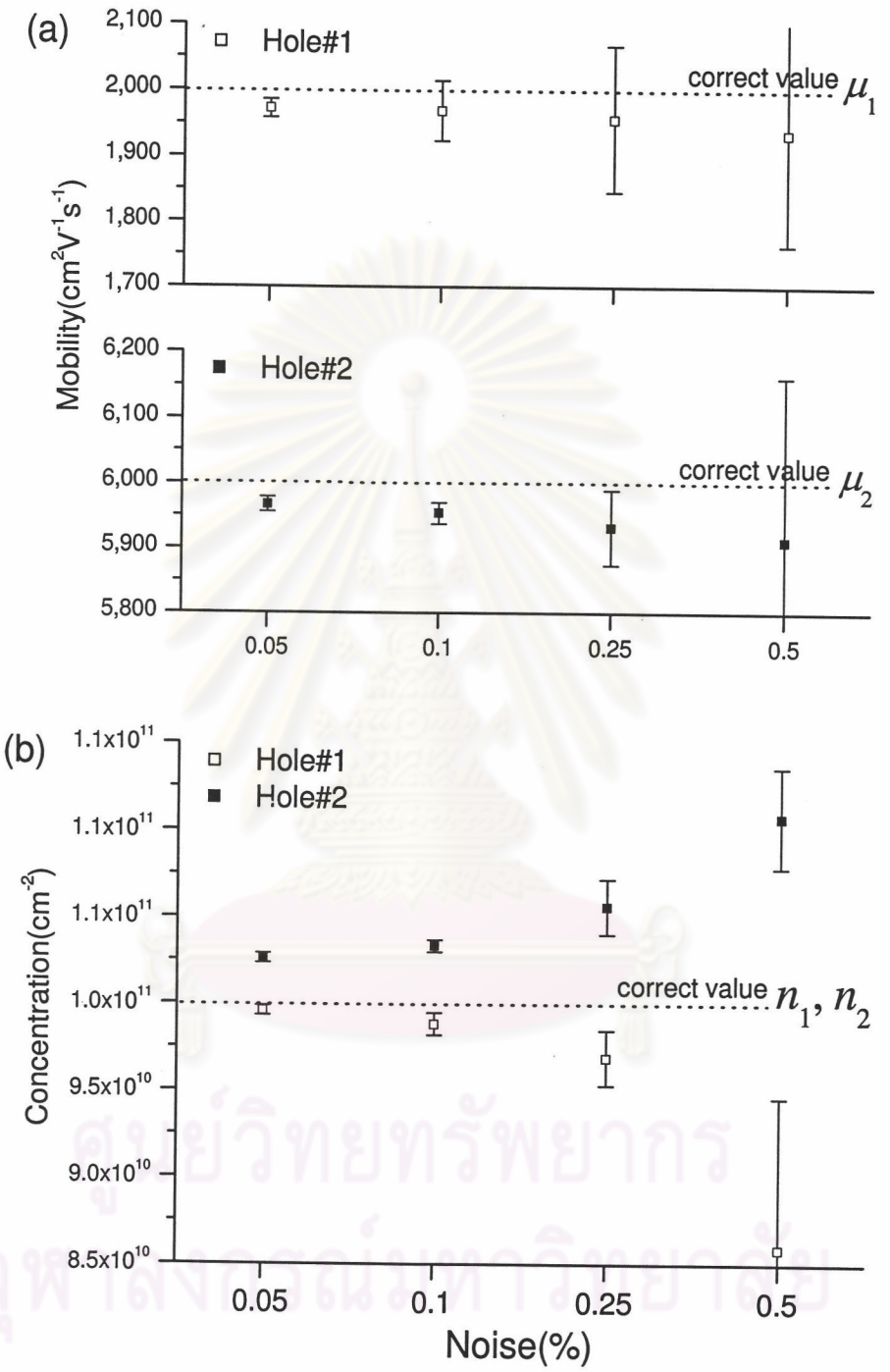

Figure 5.15: (a) Hall mobility and (b) concentration of Hole#1 and Hole#2 species at different levels of noise.

5.2 Experimental data

In this section, the magnetic-dependent resistivity and Hall coefficient of a modulation doped p-type $Ge/Si_{0.4}Ge_{0.6}$ heterostructure in the temperature range 200-300 K are employed to investigate for the temperature dependence of Hall mobility and carrier concentration. The data were collected by Kiatgamolchai et al. (2002*b*) at the University of Warvick with the superconducting magnet facility for 1,000 magnetic field points in the range 0-11 T. Within this temperature range, the Shubnikov de-Hass Oscillation was not observed and the electrical transport can be considered the classical limit.

The diagram of the sample structure is illustrated in Fig. 5.16. The virtual substrate was prepared by the Chemical Vapor Deposition (CVD) process. The sample and the subsequent layers were fabricated by the Molecular Beam Epitaxy (MBE) technique. The Ge is sandwiched between SiGe in order to produce quantum well confinement for holes near the bottom of Ge/SiGe interfaces. The boron-doped silicon germanium layer, B:SiGe, provides hole carriers. The hole carrier are transferred to the triangular quantum well in Ge layer. They are confined to transport along the plane parallel to the interface, so they are called a "two-dimensional hole gas" (2DHG). We expect to see at least two carrier species, one in the Ge channel and the other in the B:SiGe layer.

5.2.1 Calculation details

A maximum entropy mobility spectrum analysis (ME-MSA) and the Bayesian method are performed to calculate the mobility spectrum. The number of carrier species is determined, and their Hall mobility and concentration are extracted. The result from ME-MSA and Bayesian method are compared in Figs. 5.17 and 5.18 respectively.

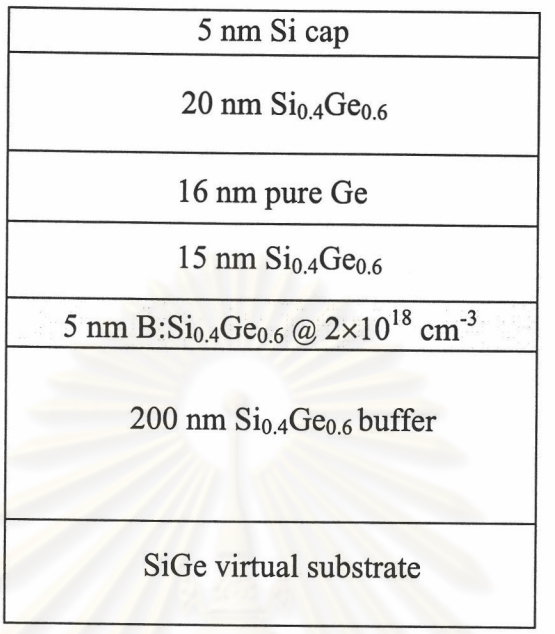

Figure 5.16: The nominal structural diagram of a modulation-doped Ge/$Si_{0.4}Ge_{0.6}$ heterostructure used in this thesis.

200 data points are selected in magnetic field range 0.5 to 11 Tesla. The mobility range is set form 100 $cm^2V^{-1}s^{-1}$ to 7,500 $cm^2V^{-1}s^{-1}$ for holes and from -100 $cm^2V^{-1}s^{-1}$ to -7,500 $cm^2V^{-1}s^{-1}$ for electrons. The ME-MSA is performed using 200 mobility points for 1,000,000 iterations with convergence parameter of 0.1. The number of mobility points used in Bayesian method are 50 points. The random noise in the measurement system is not precisely determined but can be estimated from the resolution of an equipment to be 0.1%. The Bayesian method is performed under the parameter setting shown in Table 5.9.

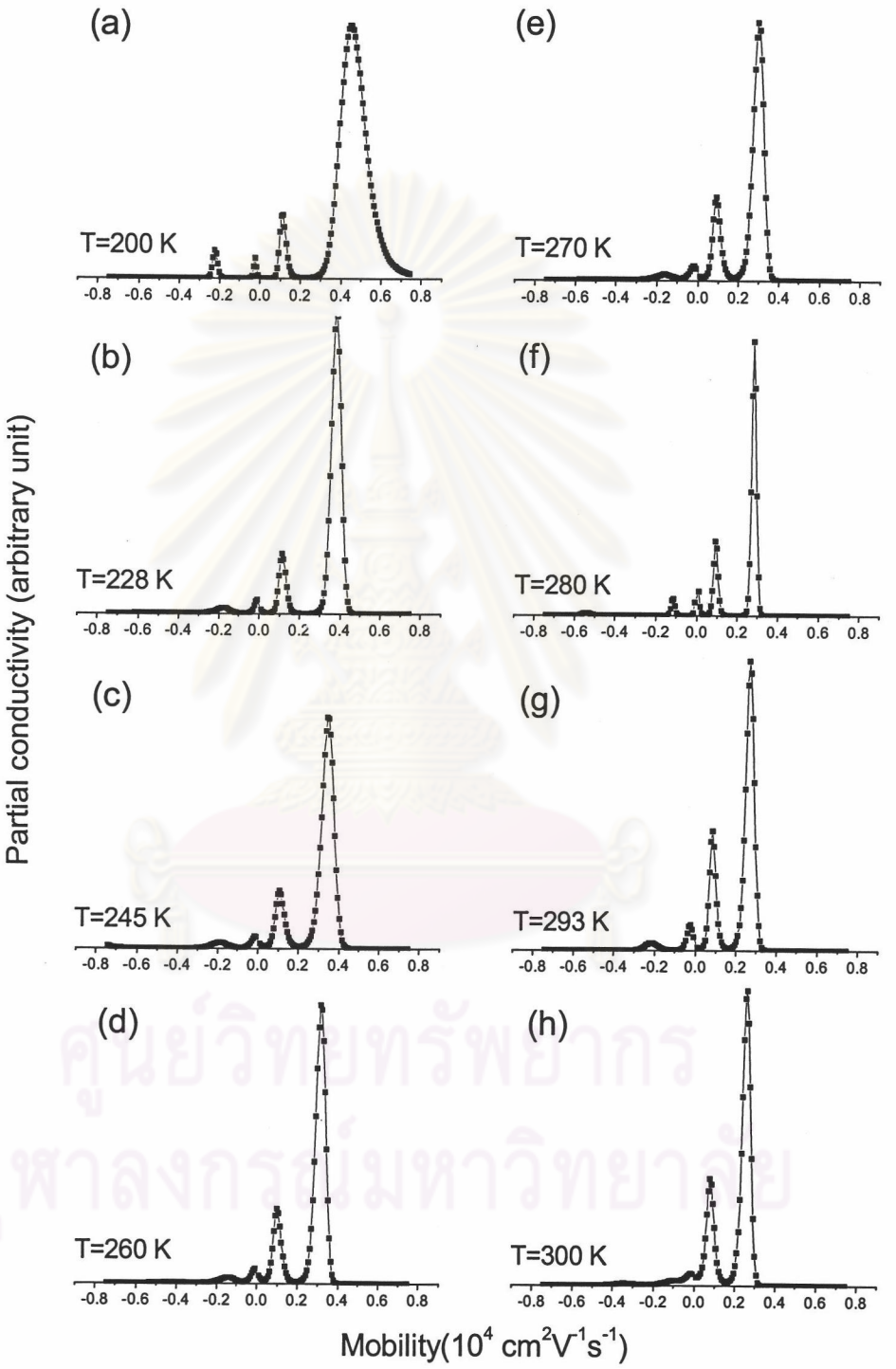

Figure 5.17: Maximum-entropy mobility spectra of $Ge/Si_{0.4}Ge_{0.6}$ in the temperature range of 200-300 K.

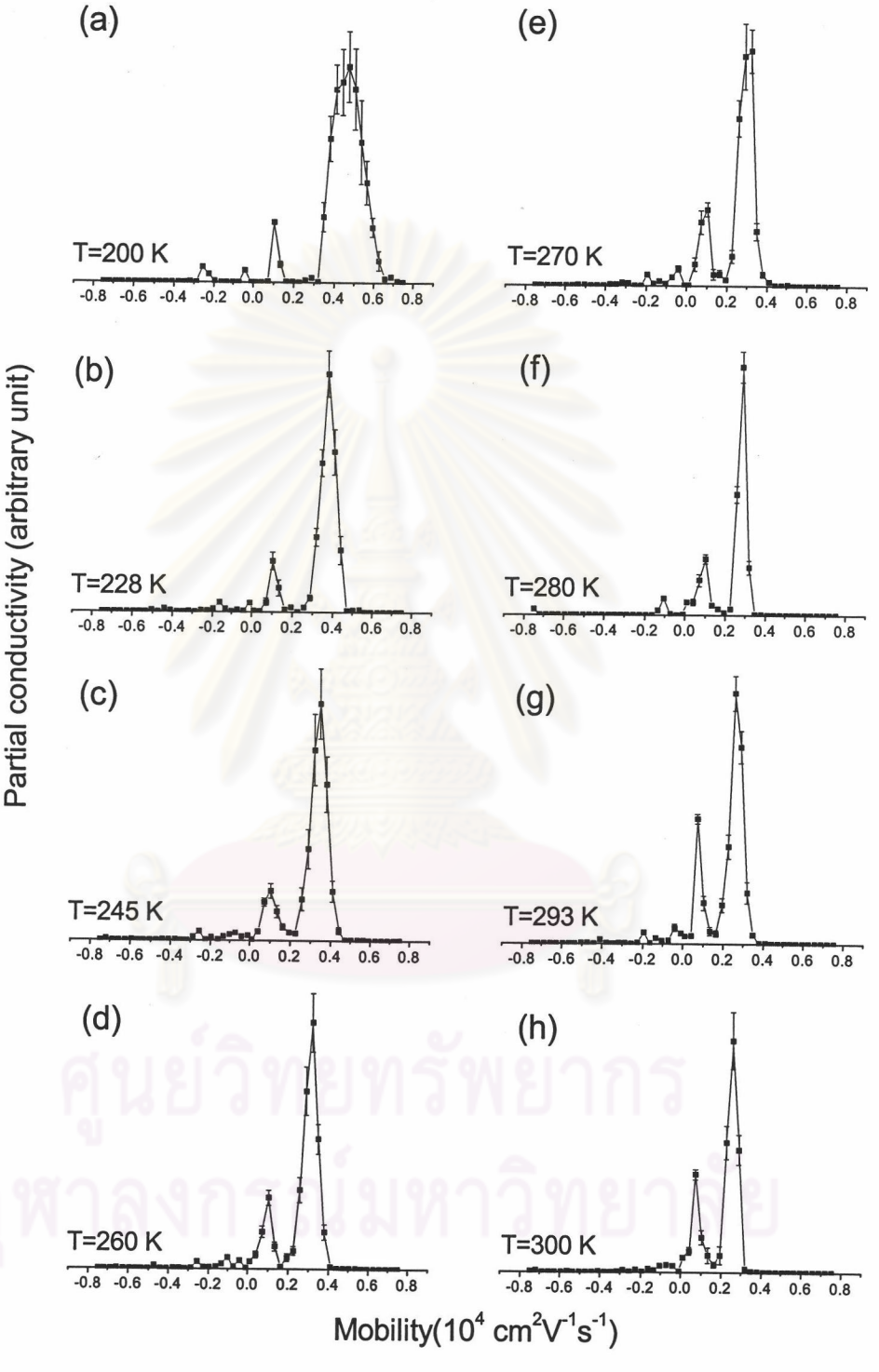

Figure 5.18: Bayesian mobility spectra of $Ge/Si_{0.4}Ge_{0.6}$ in the temperature range of 200 - 300 K.

Table 5.9 The parameter setting in Bayesian calculation on experimental data.

Configuration	Value	Range/Remark
# magnetic field points (M)	200	0.5 to 11 Tesla
# mobility points (N)	50	+100 to +7,500 $cm^2V^{-1}s^{-1}$ for hole and -100 to -7,500 $cm^2V^{-1}s^{-1}$ for electron
Default model $\{m_i\}$	Flat	
Initial α	3,600	
Decreased factor	0.9	every 200,000 iterations
Weight factor ω	1.25%	of partial conductivity
Noise (s.d.)	0.1%	of conductivity data
s.d. in likelihood	0.1%	
Stopped α	125	

5.2.2 Temperature-dependent mobility and carrier concentration of the hole species

The maximum-entropy mobility spectra (MEMS) and Bayesian mobility spectra are shown in Figs. 5.17 and 5.18. The resultant spectra from two methods are quite consistent. The spectra consist of two dominant hole peaks, a high mobility peak is 2DHG and the low one is B:SiGe, and an unknown source electron-like peak. Two hole peaks are well resolved at all reported temperatures. As the temperature increases, both hole peaks move slightly toward lower mobility. The temperature-dependent Hall mobility and carrier concentration of 2DHG obtained from both ME-MSA and the Bayesian method are shown in Tables 5.10 and 5.11, and they are plotted in Fig 5.19. For the 2DHG, the mobility decreases monotonically from about 4,700 $cm^2V^{-1}s^{-1}$ at 200 K to 2,800 $cm^2V^{-1}s^{-1}$ at 300 K, and its concentration slightly decreases form about 1.7×10^{12} cm^{-2} to 1.3×10^{12} cm^{-2}. Considering B:SiGe carriers from 200 K to 230 K, the mobility is likely to be constant at 1,200 $cm^2V^{-1}s^{-1}$. At 245 K, the mobility start decreasing, and it ends at 850 $cm^2V^{-1}s^{-1}$ at 300 K. The results from ME-MSA and Bayesian methods are slightly different at high temperature. The concentration of B:SiGe increases monotonically as temperatures increase indicating the activation of boron atoms. Although the error bar

of Bayesian value does not cover the MEMS value, the trend is approximately the same.

Table 5.10 Hall mobility and concentration of carrier species in $Ge/Si_{0.4}Ge_{0.6}$ heterostructure by ME-MSA.

Temperature (K)	B:SiGe carrier		2DHG carrier	
	mobility ($cm^2V^{-1}s^{-1}$)	concentration ($\times 10^{12}cm^{-2}$)	mobility ($cm^2V^{-1}s^{-1}$)	concentration ($\times 10^{12}cm^{-2}$)
200	1,140	0.42	4,690	1.66
228	1,150	0.66	3,790	1.46
245	1,090	0.79	3,410	1.36
260	1,020	0.91	3,120	1.29
270	940	1.01	2,950	1.28
280	930	1.01	2,830	1.25
293	850	1.26	2,670	1.23
300	780	1.48	2,550	1.27

Table 5.11 Hall mobility and concentration of carrier species in $Ge/Si_{0.4}Ge_{0.6}$ heterostructure by Bayesian method.

Temperature (K)	B:SiGe carrier		2DHG carrier	
	mobility ($cm^2V^{-1}s^{-1}$)	concentration ($\times 10^{12}cm^{-2}$)	mobility ($cm^2V^{-1}s^{-1}$)	concentration ($\times 10^{12}cm^{-2}$)
200	1,100±27	0.43±0.022	4,690±45	1.71±0.003
228	1,130±26	0.67±0.013	3,770±70	1.48±0.004
245	1,070±54	0.93±0.025	4,000±26	1.39±0.010
260	940±24	1.02±0.028	3,090±93	1.36±0.066
270	820±20	1.13±0.045	2,900±76	1.38±0.064
280	910±21	1.27±0.028	2,800±92	1.27±0.058
293	810±25	1.26±0.013	2,620±15	1.31±0.012
300	800±41	1.48±0.034	2,540±23	1.30±0.017

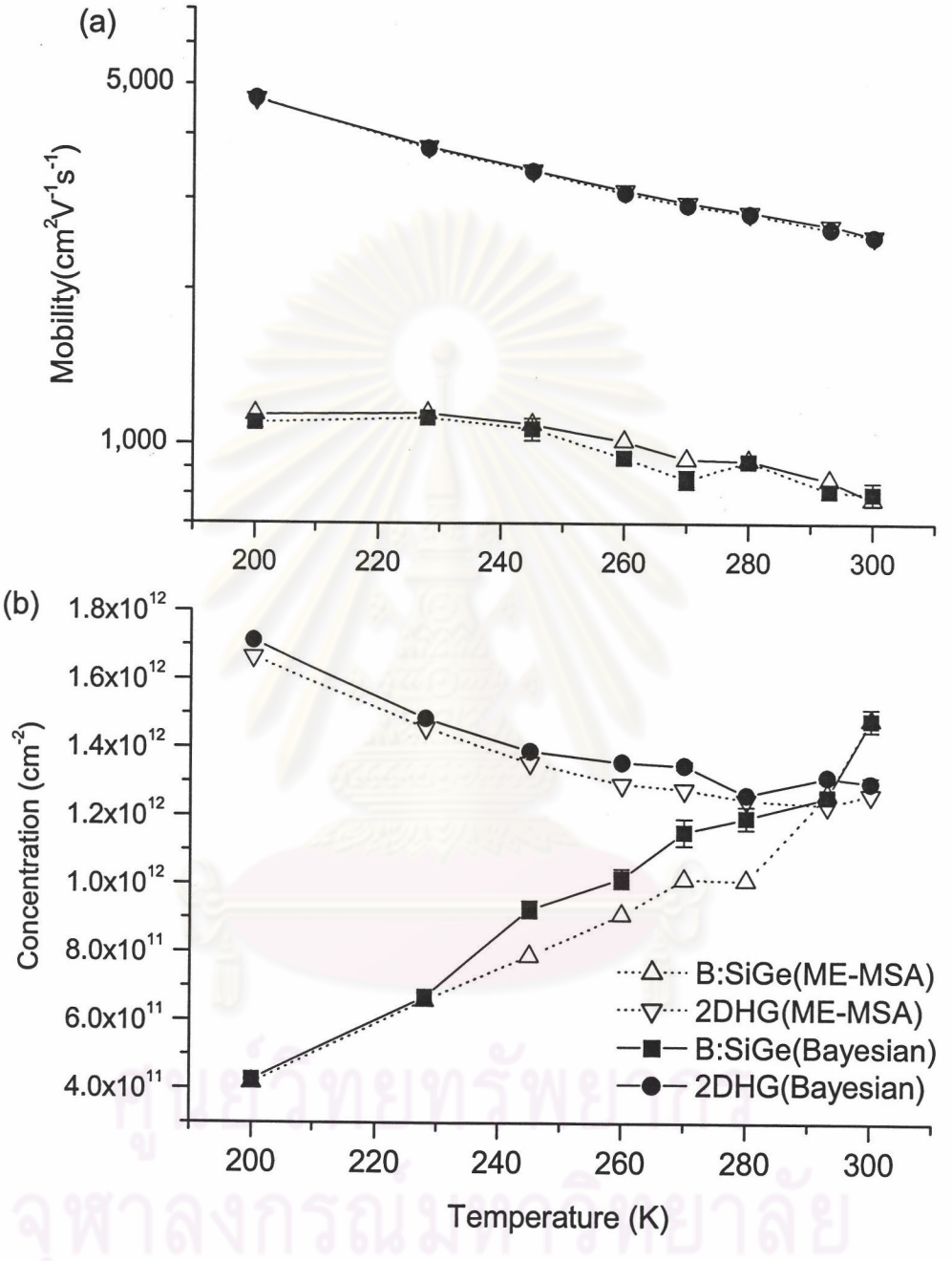

Figure 5.19: (a) Hall mobility and (b) carrier concentration of B:SiGe and 2DHG carrier species calculated form ME-MSA (hollow) and Bayesian method (solid).

The observed mobility values from the Bayesian method in the temperature range of 200-300 K are fitted to equation

$$\mu \propto T^{-n}, \tag{5.2}$$

where T is the temperature and n is a fitting parameter. Figs. 5.20 (a) and 5.20 (b) show the fit of temperature-dependent mobility of B:SiGe and 2DHG in the temperature range of 200-300 K to Eq. (5.2). The fitted values of n are 0.84±0.17 for B:SiGe and 1.53±0.02 for 2DHG respectively. For 2DHG case, it is indicated that the phonon scattering mechanism is dominant.

The activation energy E_A can be extracted from the temperature-dependent carrier concentration of B:SiGe by fitting to the following formula [Blakemore (1974)]

$$\frac{p_0\,(N_d + p_0)}{(N_a - N_d - p_0)} = \left(\frac{N_V}{\beta}\right) \exp\left(\frac{-E_A}{k_B T}\right), \quad p_0 \ll N_V \ . \tag{5.3}$$

p_0 is the carrier concentration, N_d is the donor concentration (≈ 0 for our sample), N_a is the acceptor concentration, N_V is the effective density of states in the valence band, and β is the hole degeneracy. β is set to 4 taking into account the double degeneracy of valence bandage and the spin. The fits are illustrated in Fig. 5.21. The activation energy of 138±16 meV and 174±25 meV are obtained for the result from Bayesian spectrum and MEMS respectively. The obtained results do not agree with that of Sze (1981) which reported the activation energy of B-doped Ge of 10 meV and B-doped Si of 45 meV. However, we note here that Eq. (5.3) may not be applicable for our problem because the condition $p_0 \ll N_V$ is not hold for this temperature range where N_V of $Si_{0.4}Ge_{0.6}$ is set to be 7.53×10^{18} cm^{-3} at 300 K. It is calculated by finding the weight mean between N_V of pure Si (1.04×10^{19} cm^{-3}) and N_V of pure Ge (6.0×10^{18} cm^{-3}) with weight factor of 0.4 and 0.6 respectively [Sze (1981)]. It is also temperature dependent as

$$N_V = 7.53 \times 10^{18} \left(\frac{T}{300}\right)^{1.5} . \tag{5.4}$$

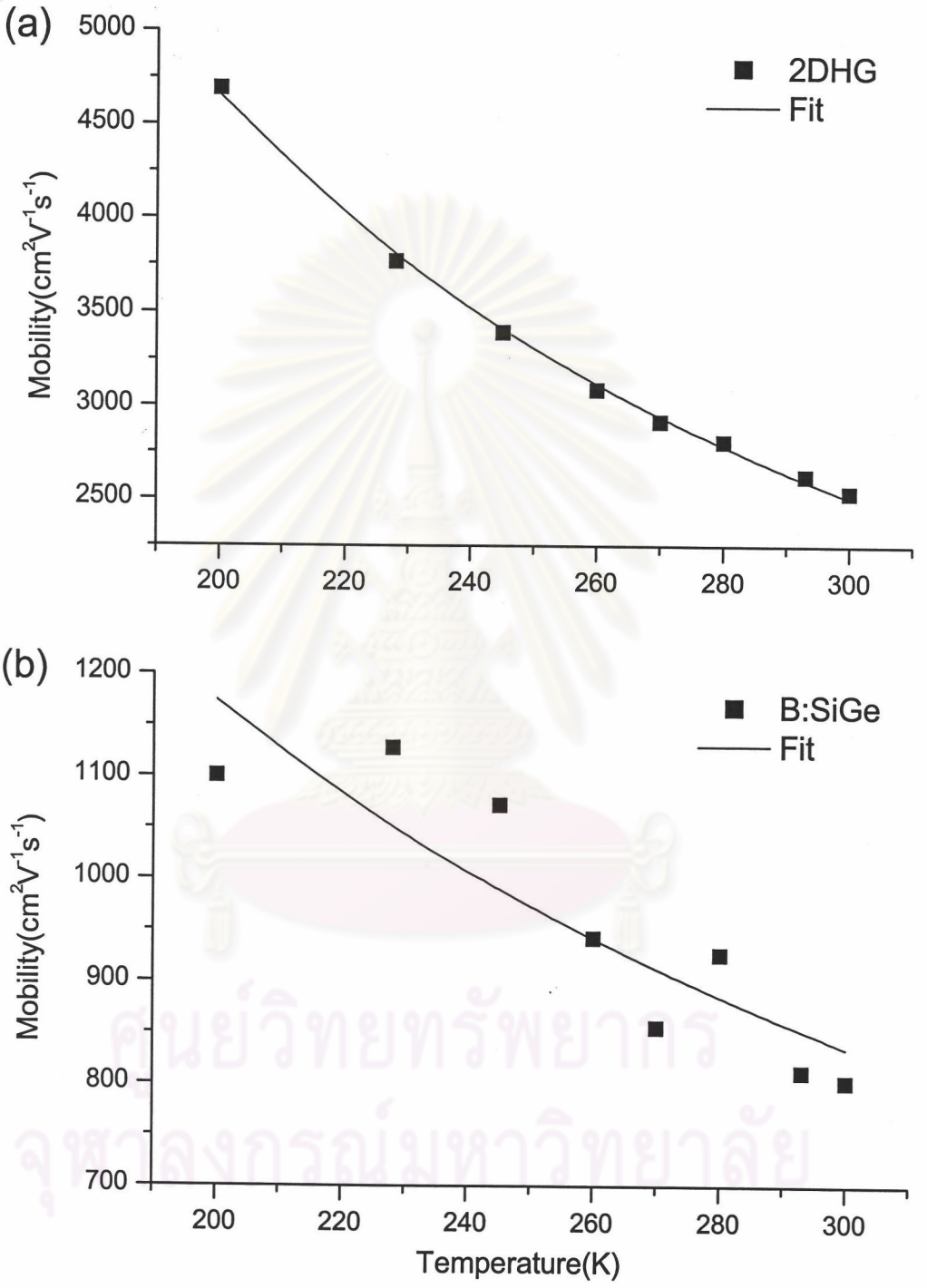

Figure 5.20: The fit of temperature-dependent Hall mobility of (a) 2DHG and (b) B:SiGe from Bayesian method.

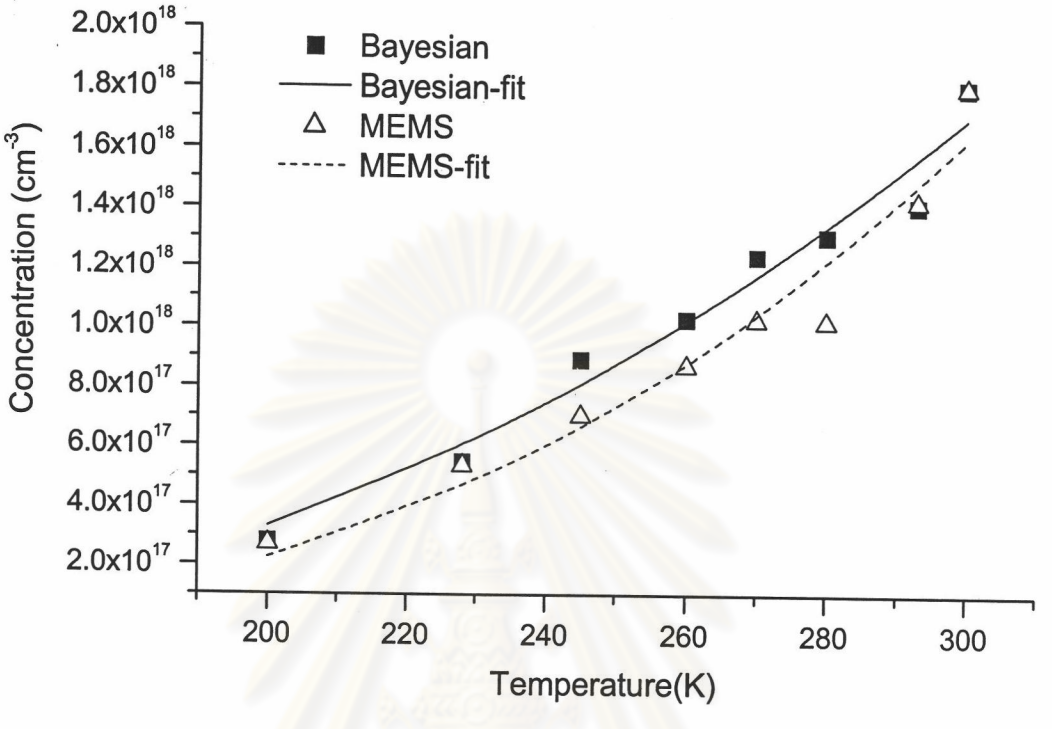

Figure 5.21: The temperature-dependent concentration of B:SiGe from Bayesian method (solid square) and Maximum-entropy method (hollow triangle). The fits are shown as solid line for Bayesian data and dash line for Maximum-entropy data.

ศูนย์วิทยทรัพยากร
จุฬาลงกรณ์มหาวิทยาลัย

5.3 Error analysis

The developed mobility spectrum calculation has been mainly concerned with the error analysis. In general, the error bar is used to represent an uncertainty of the required parameter, and the magnitude of error bar is the standard deviation of that parameter. The parameters in mobility spectrum are the partial conductivities which correspond to a differently defined mobility. By the MCMC sampling method, the mobility spectrum is represented by the member of Markov chain, a random vector of N components. In other words, a long chain is considered as a sample set of solution spectrum examined by statistical tools. Each component of spectrum has its own distribution. For example, the histogram of a selected component is shown in Fig. 5.22. Its distribution can be approximated to the normal distribution. Fig. 5.22 (a) illustrates the Markov chain, only one component at the equilibrium state. Fig. 5.22 (b) illustrates the histogram and a normal distribution. It shows that the standard deviation is reasonable to represent an uncertainty of mobility spectrum. Although the distribution of some component is not symmetric, the standard deviation still be useful to indicate roughly the deviation of that component. As a result, the spectrum uncertainty can be calculated by a statistical method. In this section, the calculated error bars are analyzed. It is clear in Section 5.1.4 that the error strongly increases following the level of noise in data. This section will show that the error bar is influenced by many factors other than the noise in measurement. A number of factors are demonstrated in order to clarify which factors affect the magnitude of the estimated error bar and how the uncertainty distribute to the parameters of each carrier species.

After the set of mobility spectrum is yielded, a statistical analysis is performed. First of all, a number of sample of each partial conductivity, s_i, are calculated for its mean and variance to form a final mobility spectrum with error bars.

By this spectrum, a number of reasonable peaks is determined to a number of carrier species within the material. Next, the total conductivity, mobility, and concentration with their error bars of each carrier species are calculated. By considering points which constitute a peak in the mobility spectrum, the required parameters are obtained using Eqs. (4.28) to (4.34). At this stage, only the uncertainty of the conductivity of each carrier species is considered. Using the propagation of error, one can show that

$$\frac{\sigma_\rho^2}{\rho^2} = \frac{\sigma_{S_{TOT}}^2}{(S_{TOT})^2}, \tag{5.5}$$

where ρ is resistivity and S_{TOT} is the total conductivity of all carrier species within the sample. The percentage error of the total conductivity is the same magnitude as the percentage error in resistivity data, so it is reasonable to use the conductivity-percentage error to study the propagation of noise in the Bayesian calculation.

In this section, we will use the spectrum of Ge/SiGe at 200K as a prototype to examine the test. Bayesian spectrum of Ge/SiGe at 200K has been calculated with 100 magnetic field points and the mobility range is extended to 10,000 $cm^2V^{-1}s^{-1}$. The spectrum is shown in Fig 5.23. From this spectrum, two dominant peaks represent two holes carrier species with Hall mobility of 1,230±30 $cm^2V^{-1}s^{-1}$ and 4,700±10 $cm^2V^{-1}s^{-1}$ and concentration of 4.65±0.02 $\times 10^{11}$ cm^{-2} and 1.667±0.004 $\times 10^{12}$ cm^{-2} respectively. The conductivity percentage error of each carrier species is 1.4% for B:SiGe and 0.13% for 2DHG. The percentage error of total conductivity, summation of two species, is about 0.08%. Even though the percentage error of total conductivity has nearly the same magnitude as 0.1% of the noise in resistivity data, it is under the question why the conductivity percentage errors of two carrier species are different by an order of magnitude. To investigate these results, synthetic data are generated using the mobility spectrum obtained in Fig. 5.23 ($Ge/Si_{0.4}Ge_{0.6}$ at 200K). It will be called the original spectrum. The data has 100 points in magnetic field range from 0.1 to 10 Tesla. The 0.1% Gaussian

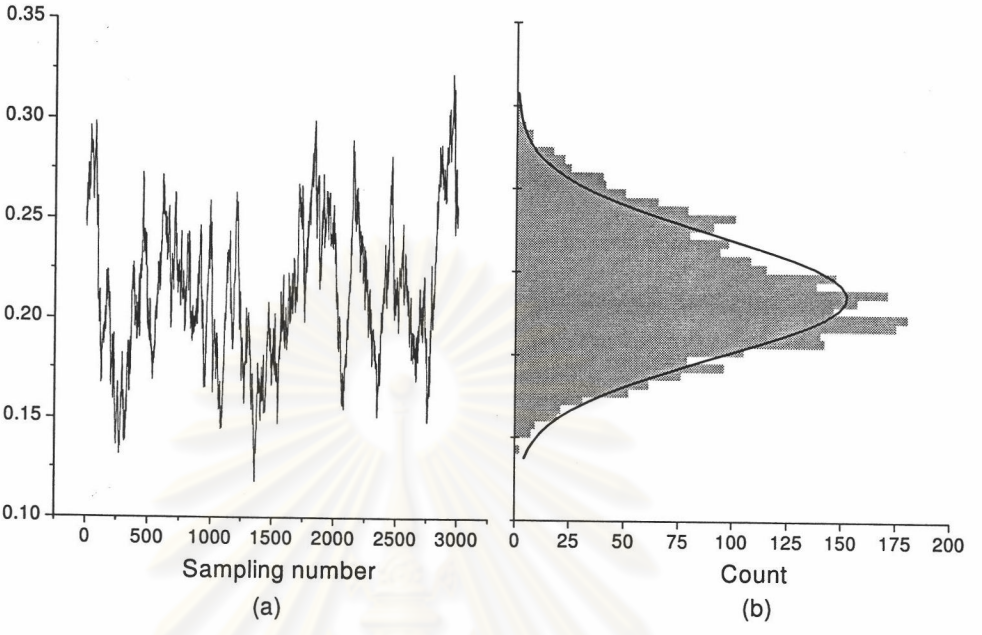

Figure 5.22: (a) A selected component of Markov chain from Bayesian calculation on synthetic data. (b) A histogram of frequency count and a fitting of normal distribution with mean and standard deviations of 0.21 and 0.037, respectively.

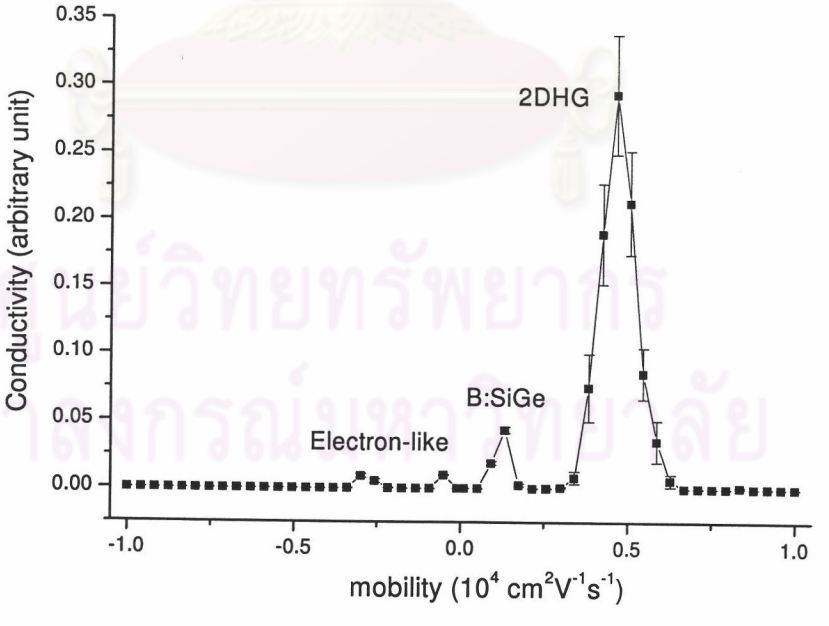

Figure 5.23: A mobility spectrum of $Ge/Si_{0.4}Ge_{0.6}$ at 200 K calculated by Bayesian method shows two major-hole peaks, B:SiGe (μ = 1,230 $cm^2V^{-1}s^{-1}$, $n = 4.65\times10^{11}$ cm^{-2}) and 2DHG (μ = 4,700 $cm^2V^{-1}s^{-1}$, $n = 1.667\times10^{12}$ cm^{-2}).

noise is added to this data and we generate 10 data set randomly.. All data set are calculated by the Bayesian method. The hypothesis is that if the original spectrum is reasonable, the repeated spectra will result in the same way. The results are shown in Table 5.12.

Table 5.12 The percentage error of conductivity of each repeated spectrum.

Data set	Error of conductivity (%)		
	B:SiGe	2DHG	Total conductivity
Original	1.39	0.14	0.08
Syn-1	2.09	0.15	0.07
Syn-2	1.78	0.11	0.06
Syn-3	1.41	0.18	0.14
Syn-4	1.81	0.13	0.15
Syn-5	2.25	0.14	0.13
Syn-6	1.57	0.11	0.07
Syn-7	1.61	0.13	0.05
Syn-8	1.88	0.16	0.18

The total conductivity percentage errors approximately match the designed value of 0.1. The B:SiGe peak has more uncertainty than a 2DHG peak for about ten times.

5.3.1 Standard deviation of likelihood distribution

The Bayesian method does not require any assumption about the number of carrier species in the interested sample. However, Bayesian calculation cannot be performed with only the measured data. It is important to know the level of noise associated within the data so that the likelihood distribution can be defined. Generally, the noise level can be estimated by considering the apparatus resolution or experiment setting. If the noise level is not reported, the width of the likelihood, a standard deviation defined in chi-square (see Eq. (4.22)), can be assigned freely by guessing; for example, most grade laboratory is set for allowing noise not excess

0.1%. This section demonstrated how the difference in assigning the likelihood width for any set of measured data affects the uncertainty in solution. Synthetic data which are generated using the original mobility spectrum in Section 5.3 is employed. The data is considered noise free, and the standard distribution defined in likelihood distribution is varied from 0.05% to 0.5%. The results are shown in Fig. 5.24 in which the conductivity-percentage errors of two hole species are plotted versus the magnitude of standard deviation. The ratio of percentage errors of large-conductivity carrier species to small-conductivity carrier species is about 10 times for all values of standard deviation. The percentage errors continuously decreases with decreasing standard deviation, and it seems to decrease toward zero if the standard deviation can be set to a very small value. In fact, decreasing standard deviation leads to a strong decreasing of acceptance rate. At 0.05% standard deviation, the acceptance rate is about 0.65% which is very low and the calculation will have to take very long time. As a result, the likelihood width should be carefully chosen. If the level of noise is unknown; in general, the standard deviation is chosen to yield a reasonable acceptance rate that is empirically suggested to be in the range of 0.5% to 5%.

5.3.2 Magnetic field strength dependency

The effect of maximum magnetic field strength to the uncertainty of solution is concerned in this section. Data set Syn-1, Syn-2 and Syn-3 in Table 5.12 with 0.1% random noise are used. These set are employed by the Bayesian method in the same way in order to treat the random effect. In each calculation, the maximum value of magnetic is set differently form 4 Tesla to 15 Tesla so that the μB is varied. The low-mobility carrier species has mobility about 1,200 $cm^2V^{-1}s^{-1}$, so the effective magnetic field strength is about 8.3 Tesla. The results are summarized in Fig. 5.25. The plot of percentage error of each carrier conductivity versus μB is shown. As the

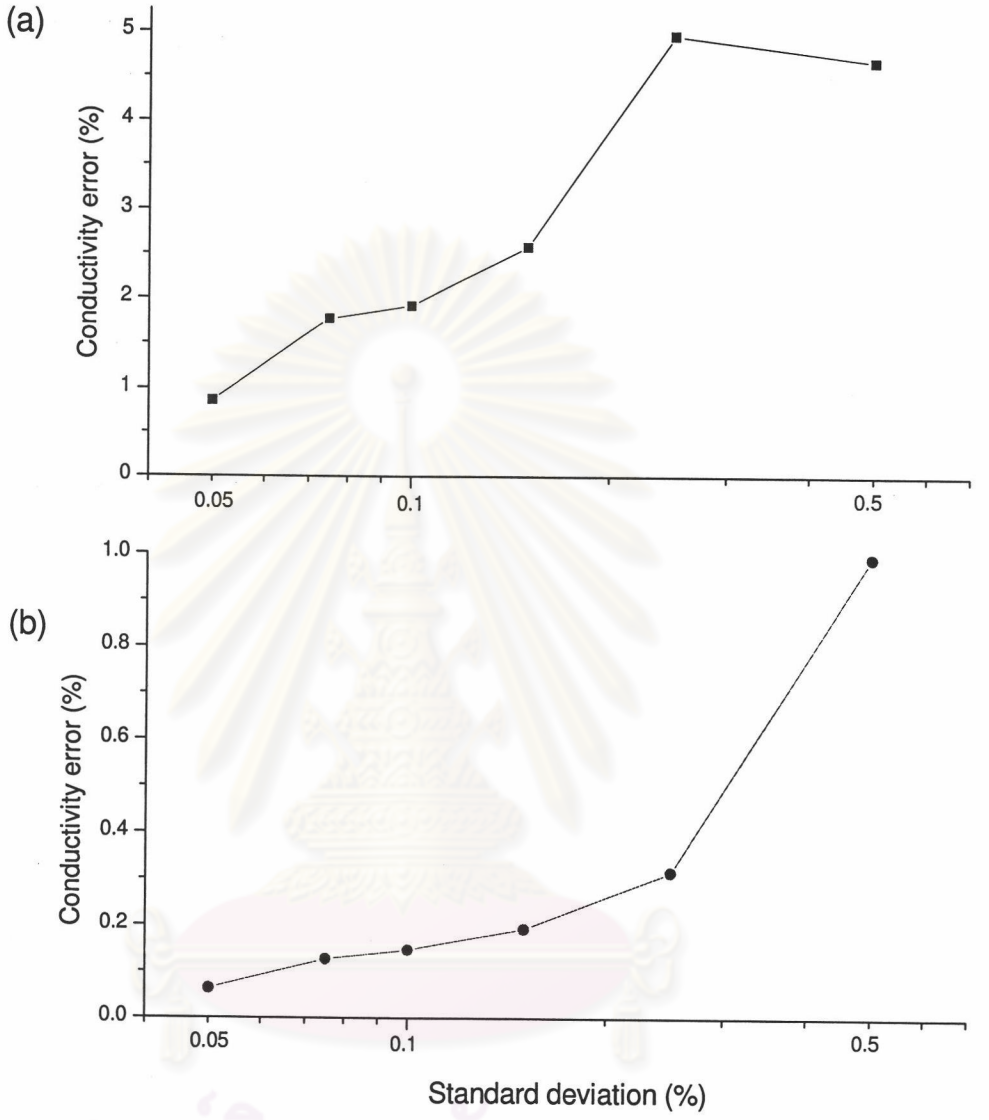

Figure 5.24: A conductivity error of (a) B:SiGe species and (b) 2DHG from synthetic $Ge/Si_{0.4}Ge_{0.6}$ data (noise free) at different standard deviations.

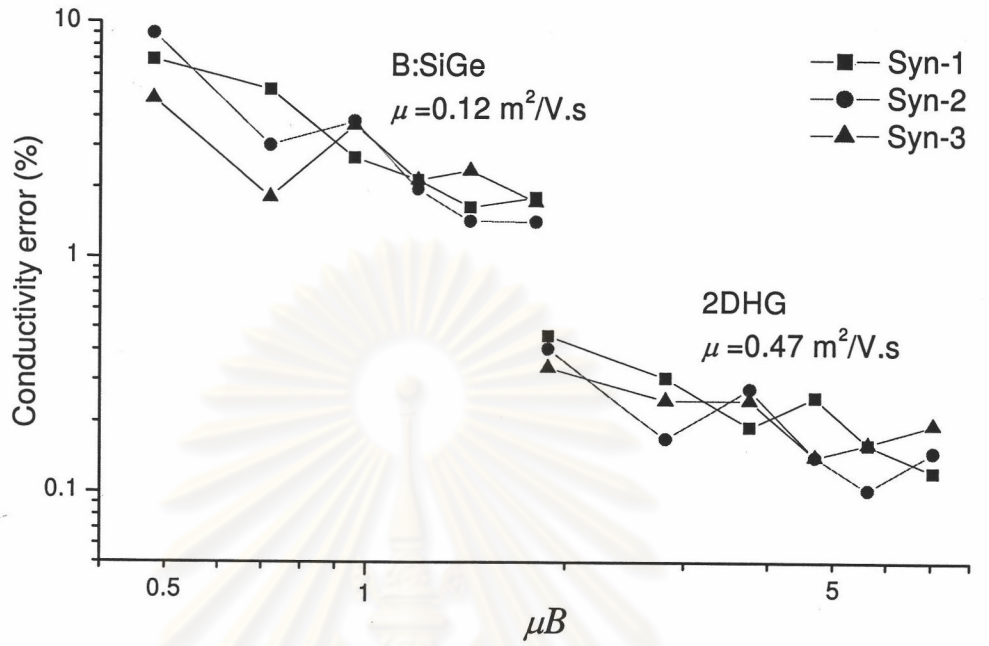

Figure 5.25: A conductivity error of B:SiGe and 2DHG species form three synthetic $Ge/Si_{0.4}Ge_{0.6}$ data (with 0.1% noise) at different maximum magnetic field strengths.

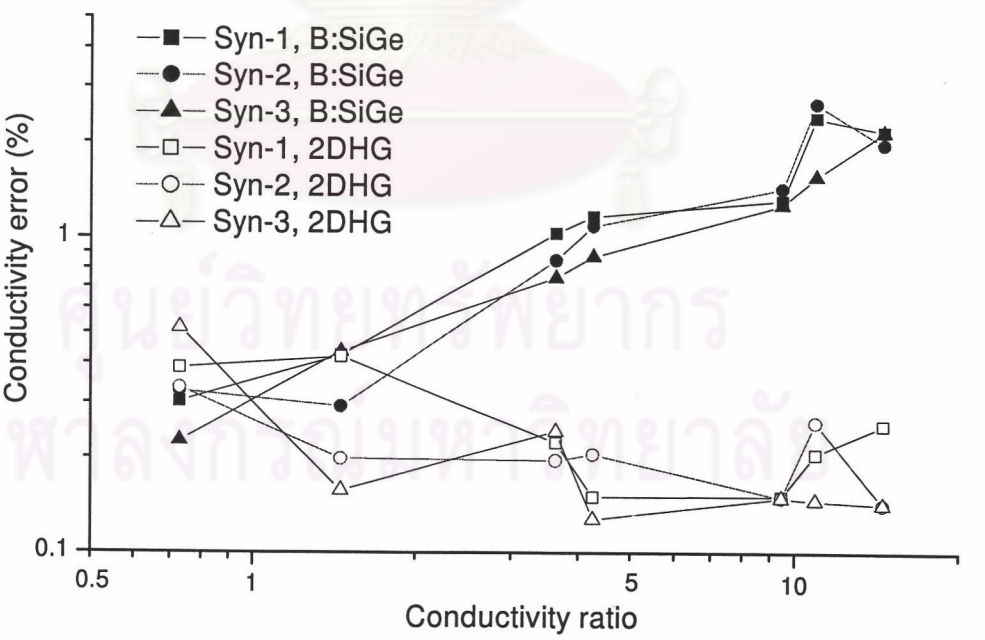

Figure 5.26: A conductivity error of B:SiGe and 2DHG species form three synthetic $Ge/Si_{0.4}Ge_{0.6}$ data (with 0.1% noise) at different conductivity ratio of 2DHG to B:SiGe.

μB increases, the percentage error gradually decreases. Even though μB for 2DHG is greater than 1 for all defined maximum magnetic fields, its uncertainly seems to relate to that of the low-mobility species. This can be summarized that the effect of maximum magnetic field is less significant when μB of the lowest-mobility carrier species becomes greater that 1.

5.3.3 The ratio of carrier conductivity

The demonstration in this section aims to clarify the different conductivity uncertainty of 2DHG and B:SiGe. Synthetic data is generated using the original mobility spectrum (original data set in Table 5.12). In this spectrum, the ratio of the conductivity of 2DHG peak to B:SiGe peak is about15 times. The original spectrum is modified in such a way that the conductivity of 2DHG is relatively decreased from 75% to 10% to its original value. So the conductivity ratio decreases. Each data set of new conductivity ratio is added with different patterns of 0.1% random noise. The results from a Bayesian calculation are shown in Fig. 5.26. The conductivity percentage error is plotted against the conductivity ratio. At the unity ratio, the percentage errors of both carrier species are equal. This indicates that the conductivity ratio is significant in distributing uncertainty to the parameters of the existing carrier species in the sample that the larger conductivity species will receive a lesser uncertainty.

In all demonstrations, we cannot precisely measure a degree of influence of each factor to the uncertainty in solution independently. However, it is helpful to examine the uncertainty obtained by the Bayesian method.